POLITECNICO DI TORINO

Master's Thesis

Membrane distillation technology in water treatment system for recirculating aquaculture system and comparison of efficiency with comparative technologies

A Thesis in the Field of Thermodynamics for the

Degree of Master of Mechanical Engineering

Author: Bilal Ahmed Khan

Student ID: S277163

Supervisor: Dr. Vittorio Verda

Tutor: Miss Chiara Iurlaro

Date: February 19, 2022

Abstract

In this era of modern technology, the need for a sustainable, green, and eco-friendly solution to the fulfilment of water needs is of the essence. Water provides energy, sustenance, and life to all living things in this world. The growth in world population, industry and domestic demand of water has increased exponentially. This has led to an increase in wastewater production, toxic and carcinogen waste being discharged into rivers, oceans, and lakes. This fact puts more pressure on the already depleting resources of fresh water in this world. Hence, there is a need to make use of fresh water more than once (recycle). This can be done by employing various technologies for water treatment and cleaning which involve different methodologies and processes.

The objective of this thesis is to analyse and perform calculations pertaining to water treatment technologies on a demo site located in Eilat, Israel. The main focus is the calculation of efficiency and other useful parameters from experimental data of the membrane distillation system that will be installed at the demo site. Other than this, other similar technologies are also reviewed, their efficiencies calculated from experimental and theoretical data for a comparison of effectiveness and efficiency among them. This approach is beneficial for choosing a more favourable system for installation.

Acknowledgement

Although my master's degree will be completed with the completion of my thesis, I hope that this lifelong path of wisdom and knowledge will continue. I owe a great debt of gratitude to Politecnico di Torino's Department of Mechanical and Aerospace Engineering (DIMEAS) for allowing me to follow my aspirations and improve my talents. For me, being a member of a multicultural institution has been a life-changing experience. During my time at Politecnico, I met some of the most creative and extraordinary people.

I'd want to express my heartfelt appreciation to my supervisor, Dr. Vittorio Verda of DENERG at Politecnico di Torino, and tutor, Miss Chiara Iurlaro, for their unwavering support and encouragement throughout my master's thesis in this unprecedented epidemic. In addition, I want to express my gratitude to my close friends Jadoon, Ifrah, Giorgia, Lodhi, Bilal, Shakeel, and Rana, who have provided ongoing encouragement and motivation throughout my master's thesis and degree.

Lastly, I want to convey my heartfelt appreciation to my parents, my aunt and siblings, who have been an integral part of my life and have always supported me. This work is dedicated to them in particular.

Bilal Ahmed Khan

Torino, January 2022

Table of Contents

List of Tables

List of Figures

List of Acronyms

MD	Membrane Distillation
DCMD	Direct Contact Membrane Distillation
SGMD	Sweeping Gas Membrane Distillation
AGMD	Air Gap Membrane Distillation
VMD	Vacuum Membrane distillation
LEP	Liquid Entry Pressure
SEM	Scanning Electron Microscopy
AFM	Atomic Force Microscopy
Kn	Knudsen number
RAS	Recirculating Aquaculture Systems
SAR	Sodium Absorption Rate
BMR	Biological Mixed Treatment
DOC	Dissolved Organic Carbon
TOC	Total Organic Carbon
MSM	Molecular Separation Membrane
TRL	Technology Readiness Level
T_{mf}	Membrane feed temperature
T_{mp}	Membrane permeate temperature
T_{bf}	Bulk feed Temperature
T_{bp}	Bulk permeate temperature
$Q_{f,conv}$	Convectional heat transfer in feed
$Q_{f,M.T}$	Heat due to mass transfer in feed
$Q_{m,cond}$	Membrane conductive heat transfer
$Q_{m,M.T}$	Membrane water vapor mass transfer
$Q_{p,conv}$	Permeate convective heat transfer
$Q_{p,M.T}$	Heat due to mass transfer in Permeate
Q_f	Volumetric flow rate for feed
Q_p	Volumetric flow rate of permeate
h_f	Heat transfer coefficient of feed
h_p	Heat transfer coefficient of permeate
J_w	Permeate flux

H_v	Enthalpy of water vapour
$H_{l,f}$	Enthalpy of the feed solution
$H_{l,p}$	Enthalpy of the permeate solution
T_{mf}	Temperature of membrane/feed interface
T_{mp}	Temperature of membrane/permeate interface
h_m	Heat transfer coefficient of membrane
k_g	Thermal conductivity of entrapped gas (air)
k_m	Thermal conductivities of the hydrophobic membrane polymer
δ	Thickness of the membrane
ε	Porosity of the membrane
EE	Evaporation efficiency
U	overall heat transfer coefficient
Re	Reynolds Number
Nu	Nusselt Number
Pr	Prandtl Number
D_h	Hydraulic diameter

1. Introduction

1.1 History of membrane distillation

Membrane distillation can be traced back to 1963 when Bodell filed for the first membrane distillation patent. Four year later, Findley published the first paper on direct contact membrane distillation. The paper included various form forms of membranes made of different materials like paper hot cup, aluminium foil, cellophane, glass fibres and nylon etc while using silicone and Teflon as coating materials to achieve the required hydrophobicity [1]. The experiments performed indicated possible economic advantages over similar technologies of the time, especially at high temperatures. The membrane life span was also a factor that increased the likeliness for the technology to be used.

This sparked a rising interest in the technology, where scientists from across the globe performed ground-breaking experiments to make the technology more accustomed and mainstream. Further patents about different schemes for the technologies were published in the following years and patents filed. Direct contact membrane distillation technologies (DCMD) enabled better ways to for recovery of demineralised water from saline solutions. Later on, after further improving on his experiments and technology, Bodell filed another patent describing his system and a procedure to convert impotable aqueous solutions to potable water. The phenomenon used air which was circulated through the lumen side and condensation of was carried out in an external tank to collect water, the experiment was the first of its kind known as sweeping gas membrane distillation (SGMD) configuration.

Initially the experiment conducted was limited to labs and other facilities but Bodell with his patent provided novel apparatus and methods to for condensing water from brine solutions, sewage urine, bacteria containing water and other polluted sourced which meant that the process could prove to be a vital source of potable water in an economical manner. Moreover, the process could be used in line with other filtration technologies like filtration in order to further improve the quality of water obtained.

The distillation process was later on introduced in Europe for desalination of seawater using the previously patented method of Bodell in the 2nd European Symposium held in Athens. It was proposed that the procedure could be utilized in cleaning of hot wastewater, and it would be possible to use it for solar distillation. But the technology quickly faded in the coming years partly due to the reason that reverse osmosis production increased significantly, whereas the production of membrane distillation reduced. But the process has significantly again increased

importance in the scientific population due to the advantages of the proficiency over its counterparts. The technology can play a vital role in the upcoming era as the world moves towards an era of water shortages, new and improved methods are more likely to be explored to their full potential.

1.2 Filtration Technologies

All filtration technologies follow the underlying principle of filtration. Filtration can be defined as a physical process that separates solid matter and fluid from their mixture with the help of a filtration medium which can have a complex physical structure through which only the liquid can pass. Diving into the types of filtration technologies, there are numerous. Most generically, the techniques can be classified into three main types as mechanical, biological, and chemical filtration. It would be not wrong to say that all these three types can be further subdivided into several sub-categories which require their own detailed explanations.

- **Membrane Distillation:**

Talking about the technology of interest, membrane distillation, is a mechanical filtration technique. The technique employs a hydrophobic membrane between the feed and permeate flow. Membrane distillation is basically a thermally driven separation process in which separation is possible due to phase change. The process can be classified as a low temperature technique. A temperature differential between the feed and permeate fluids is formed which causes a driving force to be generated across the hydrophobic membrane [2]. The MD (Membrane Distillation) separation process is then guided by vapour liquid equilibrium. The process is more energy conservative as compared to its counter parts in traditional desalination procedures [3].

Furthermore, membrane distillation can be classified into various types depending on the configuration of the system.

1) Direct Contact Membrane Distillation (DCMD)
2) Sweeping Gas Membrane Distillation (SGMD)
3) Air Gap Membrane Distillation (AGMD)
4) Vacuum Membrane distillation (VMD)

All the above-mentioned configurations differ and configuration and have their own unique use. For example, the air gap membrane distillation shown in figure 1 is more suitable for desalination and removing volatile compounds from aqueous solutions. The AGMD's design allows the feed side to only come into touch with the membrane's heated side, while stagnant air is injected flanked by the membrane and the condensation surface.[4]

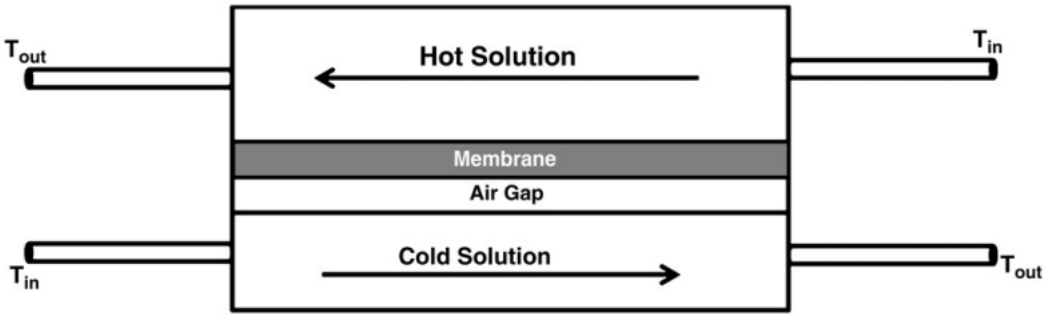

Figure 1: configuration of Air Gap membrane distillation

However, when talking about the advantages of the system, there are drawbacks present as well. Continuing on the previous example, the air gap membrane distillation helps is reducing the heat loss due to conduction, but at the same time, additional resistance is created for mass transfer due to the air gap [4].

- **Nano-filtration**

Other filtration technologies like nano-filtration and reverse osmosis are also frequently used practices for removal of salt from water and treatment of water. Nano-filtration technology relies on the difference in pressure as the main guiding power. During the transportation via the membrane, the porous nature of membrane of the membrane is responsible for the diffusive and convective fluxes taking place. The process can be said to lie between ultra-filtrations and reverse osmosis in terms of the ability to refuse molecular and ionic varieties. In fact, the nano-filtration membranes can reach up to a rejection rate of 99% for monovalent ions [5].

An advantage that nano-filtration technology has over the reverse osmosis counterpart can is the low operating pressure whereas the reverse osmosis technology requires a high pressure environment to be functional (generally speaking about 15-30 bars of pressure for brackish water and 55-70 bars of pressure foe seawater) [5]. This implies a high initial investment cost and a relatively higher energy consumption.

- **Reverse Osmosis**

Reverse osmosis (RO) is a liquid-driven membrane technique that allows water to flow through while rejecting salts and low molecular weight organic molecules [6]. With the help of an applied pressure, the osmotic pressure is overcome. Osmotic pressure refers to the colligative property that is present due to the chemical potential differences of the solvent.

The process is helpful in the removal of any types of dissolved or suspended chemicals and well as biological ones from water. The process is in use industrial processes as well as in the production of potable water.

The result of the procedure is basically that the solute is collected or is retained on the pressurized wing of the membrane while the solvent is allowed to pass through the membrane. But as mentioned above, the process requires a high differential pressure as driving force and hence needs a higher initial investment as compared to its counterpart technologies. That being said, reverse osmosis is an industrial scale process with a high efficiency capable of producing clean water among its other industrial uses.

1.3 Demo site

The Israel Oceanographic and Limnological Research (IOLR) is based in Eilat, Israel. The centre is a leading research centre that performs maricultural research focusing on marine and brackish water. Growing demand for fish product, shortage in land and water as well as environmental concerns, result in shifting aquaculture from its traditional practice and location towards implementation of recirculating aquaculture systems (RAS). The main challenges in RAS are maintaining water quality, and particularly treatment of nitrogen accumulation from protein metabolism, to enable near 100% closed loop reuse of water.

The challenge faced on the demo site includes a fish culture system that provides 250 cubic meters per hour of wastewater. Biofilters placed in the RAS are the first system of filtration to treat the water, mainly for a twostep oxidation process of ammonia, since ammonia is highly toxic to fish even at relatively low concentrations. In contrast, nitrate, which is formed when ammonia is oxidized, is less hazardous and may build in the fish-growing system to rather high levels, allowing for a significant reduction in the rate of external water exchange. Such nitrate-

rich wastewaters, which are also high in phosphorus, cannot, however, be dumped into the marine or natural environment (might cause eutrophication).

Nonetheless, neither for marine RAS nor for sea water desalination facilities, efficient and cost-effective methods for nitrate removal from marine wastewater have been well established. As a result, rather than dilution, brine and effluent from desalination facilities and land-based fish farming RAS are dumped directly into the sea.

An additional problematic issue related to recirculation of aquaculture systems is the need to disinfect the effluent, since it adds operational cost that might reduce the profitability of production. Reducing the effluent flow rate (by reducing the external water exchange rate) would reduce disinfection costs, however, very low water exchange rate will result another constrain of accumulation of fine size suspended solids (less than 15 μm) that deteriorate internal water quality for fish growth. Other issues preventing the 100% recirculation of the water in the RAS are related to the values of salinity and biological oxygen demand (BOD), that easily grow in fully closed recirculated marine fish culture systems.

The main goal for this demo site from the technological point of view is to establish a feasible water recycling cycle for the land-based marine aquaculture system in a cost effective and environment friendly way. The technology module developed for this purpose is called SALTECH (treatment module for salty water). The following figure depicts the technologies that are part of the technological loop in order to clean the water and reuse it for other purposes including drinking.

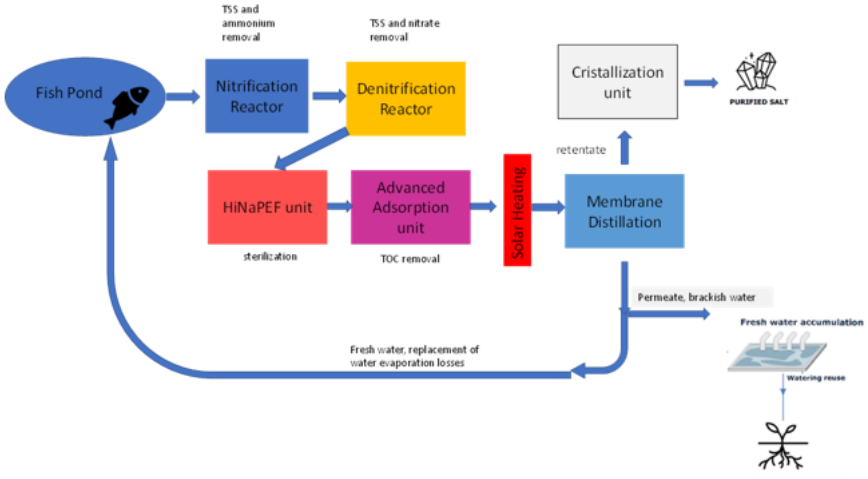

Figure 2: Demo site 2 train of technologies

The train of technologies include various systems such as Adsorption unit, a generator capable of producing electric pulses for the sterilization of water, a denitrification unit for removal of nitrates, solar heating before the membrane distillation unit to reach an optimal temperature. However, the main discussion for this thesis is the membrane distillation unit that is responsible for removal of water vapours from the retentate which is later sent to the crystallization unit to convert the retentate to purified salt crystals. To maintain the loses of water due to evaporation during the whole procedure, fresh water is introduced into the system to maintain a level of input for all the technologies for them to work in a feasible range in which they are efficient.

Coming to the focused technology in this thesis, the membrane distillation prototype experiments were performed in collaboration with the university of Aalborg, Denmark. The nano-filtration data has also been obtained from the same source. The generator called high voltage nano second pulsed electric field generator (HVNSPEF) manufactured for producing high voltage for water sterilization, its data was obtained from IRIS s.r.l., the generator is also being used at the demo site for purification purposes of incoming supply of water. The data extrapolated from the experiments is the basis of the calculations there will follow. The membrane distillation technology, as mentioned previously is a good alternative for the reverse osmosis technology, especially in terms of cost effectiveness as it does not require a huge initial investment for machinery to be installed and is easier in terms of maintenance as well.

1.4 Definition of the Problem and Objective of the Thesis

Over the last several decades, the spread of various technologies in the water treatment and filtration sector has resulted in a multi-fold rise in chances for recycling brackish and salty water that was previously unsuitable. This creates a huge opening for companies, firms, and regulatory bodies alike to benefit from these modern technologies. New and modern research is being carried out to figure out the compatibility of each technology in liaison with the existing inline methods previously used.

This being said, modern technologies connected in in such a way that they are able to provide better water treatment solutions in a more cost effective and efficient manner are also a very attractive option. Different configurations of technologies, having their own pros and cons are being compared to check whether the technology in question is a better fit for the problem in hand or an alternative might be considered.

Membrane distillation is one of these technologies which are under consideration. With its various configurations and working conditions, the technology is able to serve various industries depending on their requirements and needs. The objective of this thesis is then to understand the working of this technology, the principles of thermodynamics and fluid mechanics that the technology follows and adapts to perform its sole task of distillation.

The membrane distillation unit installed in the demo site in Israel is basically to reduce the salinity of water. The salinity of water is measured by the amount of conductivity the sample offers when a current is passed through electrodes placed inside the sample. The lower the conductivity value, the lower the salinity of the sample meaning that the sample is hence cleaner and does not contain salt compounds that might be harmful to reuse if the sample is to be recirculated for various uses in industry or even domestically. It is worth mentioning that apart from the salinity of water, there are other indicators such as pH value etc that are also checked to make sure that the sample is absent of other impurities as well.

The objective of this thesis includes the calculation of the efficiency of the system using MATLAB. The analysis calculates the evaporation efficiency of the system using the experimental data obtained from the university of Aalborg, Denmark. Other than that, the analysis is to include the temperature polarization coefficient which is also an indicator of efficiency as the system is incredibly prone to polarization of temperature phenomenon, which is discussed further in literature review.

To carry out this analysis to calculate the evaporation efficiency and temperature polarization coefficient, various unknowns that are required are also found using the MATLAB software. Therefore, with the focus on thermodynamic side of the system, we try to analyse two efficiency indicators of the system irrespective of the other indicators which focus more on the cleanliness of the permeate that is obtained during the whole process.

The thesis also includes a detailed comparison of the technology under question with similar technologies being used in the demo site itself. The technologies are nano filtration, separation of ions by passing current at extremely high potential difference, and reverse osmosis (which is not part of the demo site but a similar technology).

1.5 Thesis Outline

The thesis consists of eight chapters. The first chapter "introduction" entails a brief overlook of the membrane distillation history, the filtration technologies, the demo site where the system is to be installed, and the highlights the problem definition and the objectives of the thesis. The second chapter is dedicated to the present literature review associated to the topic of symposium and theoretical background with the emphasis on thermodynamic and fluid mechanic indicators and linked literature related to the performance of the system. In the third chapter, the methodology of the approach that is taken to calculate the above-mentioned indicators is discussed in detail along with the possible demo site developments. After the theoretical aspects are discussed, a mathematical model that was used for the calculations to be performed in MATLAB® is extensively discussed. The fifth chapter includes a detailed calculation of the experiments conducted on the technology under discussion among its counterparts that are available in the market. This involves a common parameter to be examined among all the technologies in question and then discuss whether if the system is well designed to maybe the alternative technology would perform better under given circumstances. The discussion includes the working principles of the alternative technologies and their pros and cons as compared with membrane distillation. The sixth chapter includes the comparison of the similar technologies. The seventh chapter talks about the SEC value comparison and finally the last chapter is on discussions and results in the form of conclusions obtained from the calculations of the efficiencies. The recommendations to improve on the existing model or the use of some other alternative configuration is also debated. The outline of the thesis is shown in figure 3.

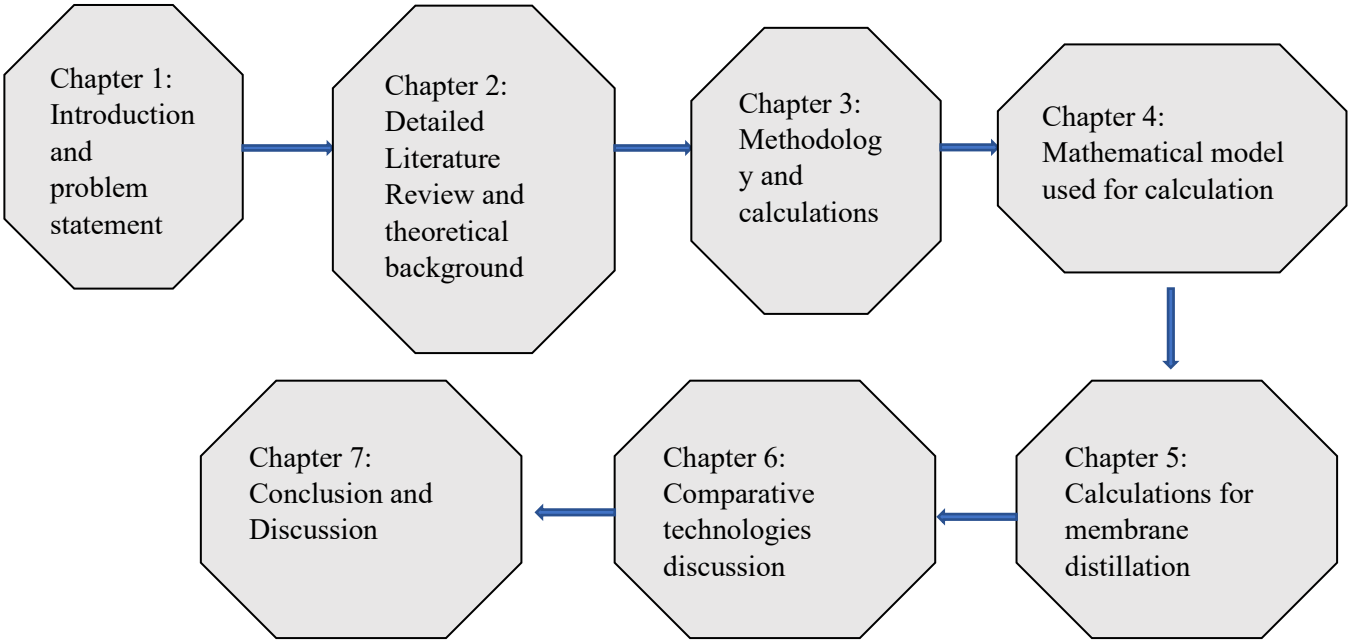

Figure 3: Outline of the Thesis

2. Literature Review and Theoretical Background

This chapter entails the discussion about the literature review carried out about the system under consideration i.e., membrane distillation. Suggested research articles are read, demonstrating the technology's essential use in the industry. It's worth noting that membrane distillation research began in the 1960s but came to a halt in the middle due to fast breakthroughs in other related technologies at the time. There is still a lot of study being done on the integration of technology with different other technologies. The following graph about the research on membrane distillation technology portrays the above-mentioned phenomenon quite well.

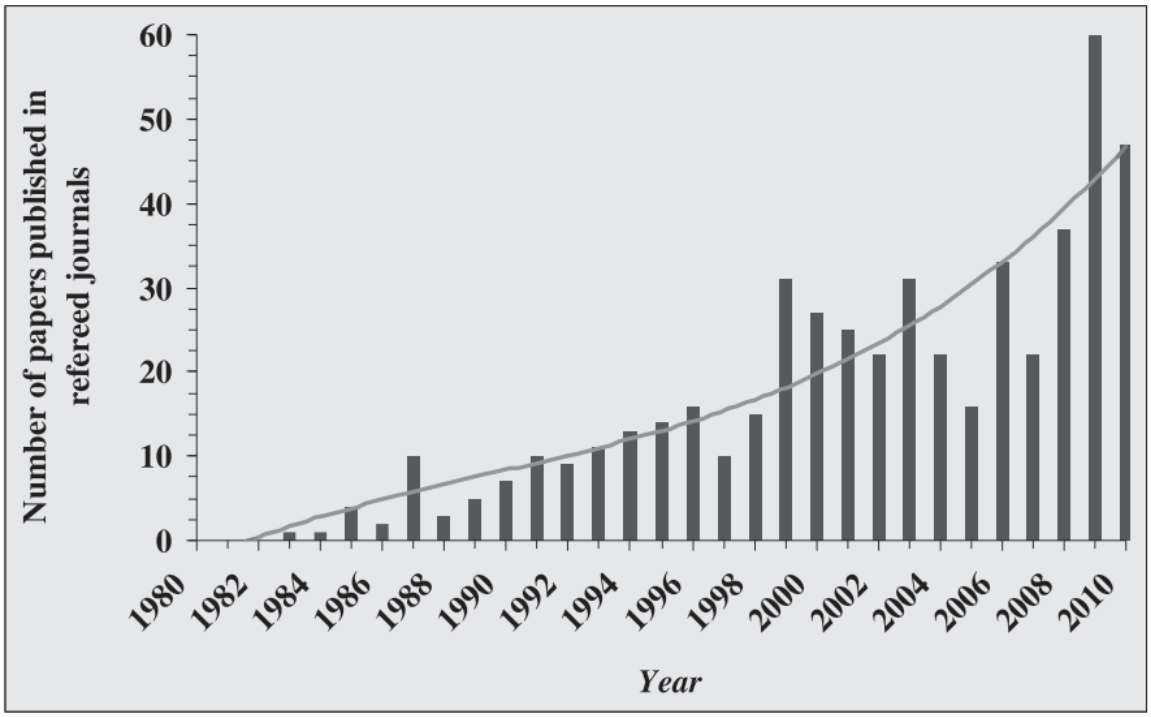

Figure 4: Up until 2010, the growth of research MD activity was depicted as a plot of the number of articles published in reputable journals for each year[1].

Furthermore, the literature then splits into various categories talking about the different aspects of the technology. Papers split into the chemical part of things as well as the mechanical and thermodynamic part of the problem. Talking about the thermodynamic and fluid mechanic side of things, the literature gets more focused on the heat and mass transfer phenomenon. How the two phenomena are root basis for the whole system to perform. Before getting into the details of the efficiency factors of the membrane distillation, it is vital that the thesis establishes a base of the other parameters involved in the calculations of the efficiency. But to discuss the

efficiency of the system, we first discuss the first law of thermodynamics to further get into depth of the details of the efficiency.

2.1 Efficiency of a system

The first law of thermodynamics states that the energy of a system is conserved. It can be converted from one form to another, but it is never destroyed or lost. The ratio of usable energy given to the job to the needed energy input may be thought of as the first law efficiency of an activity in its most basic form [7]. If we consider a mass of gas enclosed inside a cylinder fitted with frictionless piston at a persistent temperature, and an amount of heat q is applied to the system. Due to the heart being absorbed by the gas inside the cylinder, the gas performs the work w by expansion. So, following the first of thermodynamics, we obtain the following equation:

$$\Delta U = q - w \quad (1)$$

Where ΔU is the increase in the internal energy of the system. This above-mentioned equation can be regarded as the basic mathematical expression for first law of thermodynamics [8]. The first law efficiency is a then a ratio of the output work produced, and the input energy provided. Mathematically, it can be written as the following:

$$\eta = \frac{work\ output}{energy\ input} \quad (2)$$

The efficiency of the system is inversely proportional to the energy loss of the system. The less the energy being lost or wasted, the greater the amount of efficiency of the system will be. The first law of thermodynamics tells us about the conservational nature of energy, that it may be converted from one form to another, and it cannot be destroyed.

But intuitively, we are familiar that something is lost when a full tank of petrol is combusted to produce work, or when a meal is consumed. That something lost is exergy – which can be thought of as the capacity of energy to do work. To define the exergy phenomenon, it can be said that the exergy of the system or a resource is the maximum work that a system can produce as it comes into equilibrium with the environment.

When we talk about efficiency of membrane distillation, we talk about the energy of the system in terms of heat transfer. The heat transfer mechanism of membrane distillation then also entails elements of mass transfer. In its most basic form, efficiency in membrane distillation can be thought of as the amount of heat transferred to the maximum amount of heat that could be

transferred. Of course, the two values differ due to loses depending on various parameters including the configuration, the amount of conductive heat loss to name a few.

2.2 Membrane Distillation

2.2.1 Membrane Configurations

This section caters for the detailed analysis of the various membrane configurations in the membrane distillation technology. Different membrane configurations are used for separation of different kinds of aqueous solutions using microporous hydrophobic membranes. The explanation of these membrane configurations are as follows:

- **Direct Contact Membrane Distillation (DCMD)**
  In membrane distillation, direct contact membrane distillation is the most common design. The hot feed solution is in direct contact with the membrane's hot side surface in this setup. [4]. The principle of mass transfer is the pressure difference created across the membrane on the permeate side. This pressure difference causes the vapour to move across the membrane towards the permeate side and to condense. The fact that the membrane is hydrophobic, holds back the liquid on the feed side from entering the membrane and move to the permeate side (meaning only gas phase can exist inside the membrane pores). Direct contact membrane distillation has a one major flaw that is heat loss by conduction. The following figure depicts the configuration of the membrane more explicitly.

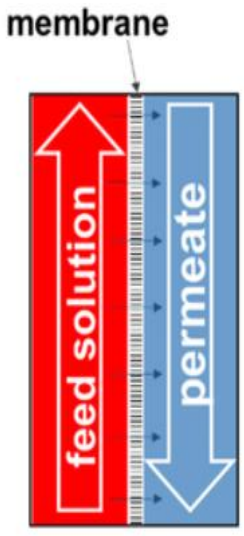

Figure 5: Depiction of Direct Contact Membrane Distillation Configuration

As shown in the figure, the direction of the feed and permeate solution is not the same rather counter to each other. This helps in a better heat transfer from the hot feed solution to the permeate solution.

- **Air Gap Membrane Distillation (AGMD)**

  Air gap membrane distillation is a configuration of the membrane distillation technology in which the hot feed solution is in direct contact with the membrane only while an air gap is maintained between the permeate fluid and the membrane. The configuration, as shown in figure 1, helps in a reduced heat loss by conduction. The stagnant air gap created among the permeate flow side and the membrane aids vapour in crossing over and condensing on the permeate fluid's chilly surface. However, even though the heat loss by conduction is reduced from such a configuration, the mass transfer resistance is now higher due to the air gap introduced, which puts this configuration at a disadvantage. Some industries use this kind of configuration in order to remove volatile compounds from aqueous solutions [9].

- **Sweeping Gas Membrane Distillation (SGMD)**

  This membrane distillation design consists of a sweeping gas as the permeate at the permeate flow side. The inert gas is responsible for sweeping the vapour from the permeate side of the membrane module and causing it to condense outside of it. Alike the air gap membrane distillation technology, the sweeping gas also has an air gap, although not stationary which helps increase the mass transfer coefficient. The fundamental disadvantage of this arrangement is that a little volume of permeate diffuses owing to the high volume of sweeping gas, necessitating a bigger condenser in order for the system to function. The configuration of membrane distillation technology is shown in the diagram below.

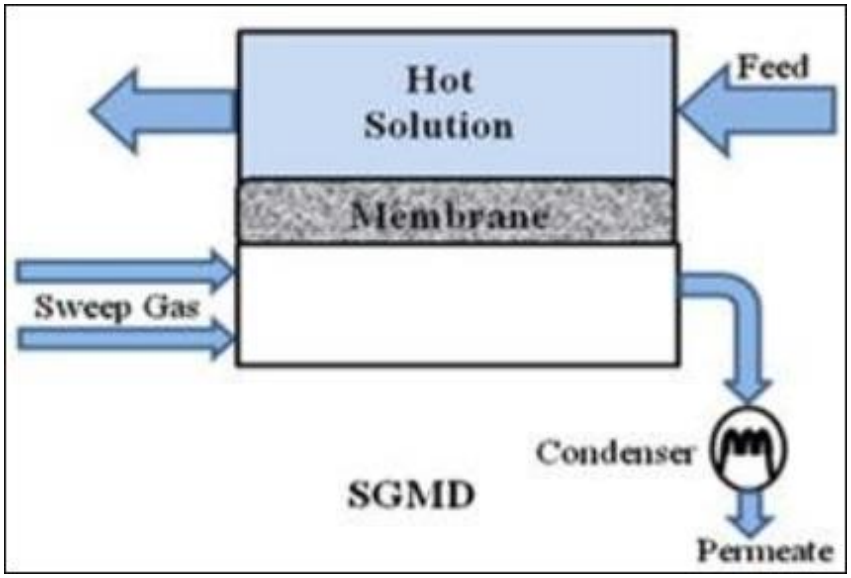

Figure 6: Configuration of Sweeping Gas Membrane Distillation

It is also worth mentioning that the above mentioned two technologies that are air gap membrane distillation and sweeping gas membrane distillation can also be combined to form another type of distillation process which is known as "Thermostatic Sweeping Gas Membrane Distillation" (TSGMD). The inert gas is passed through the membrane and the condensation surface in this circumstance. A portion of the vapour condenses on the condensation surface (AGMD), while the rest is condensed by an external condenser outside the membrane cell (SGMD). [10]

- **Vacuum Membrane Distillation (VMD)**

  A vacuum is created in the permeate membrane side of a VMD configuration using a pump. Outside of the membrane module, condensation occurs. The amount of heat lost by conduction is small, which is a significant benefit.[11] The vacuum membrane distillation is also used for separating aqueous solutions and volatile compounds. The following figure depicts the vacuum membrane distillation configuration for a better explanation.

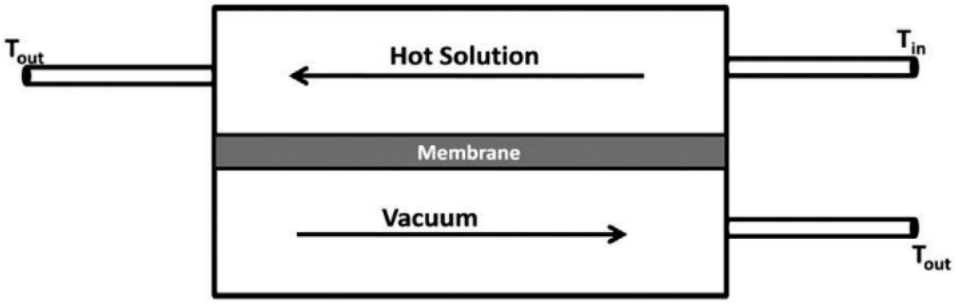

Figure 7: Vacuum Membrane Distillation Configuration

2.2.2 Membrane Characteristics

The most important part of the membrane distillation technology is the membrane itself. The membrane is a hydrophobic (non-wetting) porous structure made from polytetrafluoroethylene (PTFE), polypropylene (PP) or polyvinylidene fluoride (PVDF). The key feature of all of these materials is their low mass transfer resistance and thermal conductivity, which allows the system to experience little heat loss across the membrane. The membranes must also be able to function under harsh temperatures, which means they must be thermally stable and chemically resistant.

Some of the important characteristics of the membrane are discussed below:

- **Wetting Pressure or Liquid Entry pressure**

  The liquid entry pressure (LEP) is one of the most significant characteristics of the membrane. The membrane pores must not get wet from the feed liquid, or in other words the feed liquid should not be able to penetrate the membrane pores. This means that the LEP is the maximum pressure limit that the membrane can handle and hence the applied pressure should not exceed the LEP in order for the membrane to stay hydrophobic. Studies have shown that the LEP is directly related to the feed concentration and presence of organic solutes, which aid in reducing the LEP [12]. Further research on the topic also concluded that the LEP is also strongly dependent on the type of concentrations in the feed e.g., LEP was studied to be linearly decreasing when the ethanol concentration in the solution was increased. The formula to calculate the decrease in pressure was published by Franken in his paper about the wetting criteria

applicability of the membrane distillation. According to him, the LEP can be estimated according to the following formula:

$$\Delta P = P_f - P_p = \frac{-2B\gamma_l cos\theta}{r_{max}} \quad (3)$$

In the above equation, the pressures P_f and P_p represent the pressures of the feed and permeate side respectively, B represents the geometric pore coefficient (which is 1 for cylindrical pores), γ_l is the liquid surface tension, θ represents the contact angle and r_{max} is the maximum pore size.

The influence of salt content on water surface tension may be quantitatively described as in relation to the surface tension at standard temperature and pressure.

$$\gamma_{l\_new} = \gamma_l + 1.467c_f \quad (4)$$

Where γ_l is the surface tension of pure water at 25°C, which comes out to be 72mN/m. Hence as a result, membranes that have a higher contact angle (meaning high hydrophobicity), smaller pore size, low surface energy and high surface tension for a feed solution have a higher LEP value. According to literature, typical pore size to prevent wetting can range from 0.1-0.6μm.

- **Membrane Thickness**

Membrane thickness is a significant trait of the membrane distillation system. The permeate flux and the membrane thickness are inversely proportional to each other. This is because the permeate flux decreases as the membrane thickness increases due to the fact that the resistance for the mass transfer increases. Inversely, the heat loss reduces when the thickness of the membrane is increased. So there a is trade-off involved between the choice of increased mass transfer or heat loss. The membrane thickness has been thoroughly studied theoretically by Lagana [13]. They concluded that the optimal range of membrane thickness is between 30-60μm. It is to be noted that in AGMD the membrane thickness can be neglected because of the stagnant air gap that exists between the permeate flow and membrane as it is the dominant factor of resistance to mass transfer.

- **Membrane porosity and tortuosity**

The void volume fraction of a membrane (defined as the volume of the holes divided by the overall volume of the membrane) is known as membrane porosity. Membranes with a higher porosity have a bigger evaporation surface area. To calculate membrane porosity, two kinds of fluids are employed. The first (for example, isopropyl alcohol, IPA) penetrates the membrane pores, but the second (for example, water) does not. A membrane with a high porosity has a greater permeate flow and less conductive heat loss in general. The Smolder–Franken equation [14] may be used to calculate porosity (ε).

$$\varepsilon = 1 - \frac{\rho_m}{\rho_{pol}} \quad (5)$$

In the equation, the ρ_m and ρ_{pol} are the densities of membrane and polymer material respectively. According to a study, the membrane porosity of a system varies from 30 to 85%.

The divergence of the pore structure from a conventional cylindrical form is known as membrane tortuosity. Tortuosity and permeate flux are inversely related, indicating that the larger the tortuosity, the lower the permeate flux. One of the most lucrative formulas to calculate the tortuosity relation was suggested is the following [15]:

$$\tau = \frac{(2-\varepsilon)^2}{\varepsilon} \quad (6)$$

- **Thermal Conductivity**

Two of the main factors that contribute to the calculation of thermal conductivity are thermal conductivity coefficients of polymer k_s and gas k_g respectively. The value is dependent on temperature, the degree of crystallinity, and the shape of the crystal. Usually, the thermal conductivities of most hydrophobic polymers are quite close to each other. For example, the following table represents the thermal conductivities of the hydrophobic membranes at 23^{O}C.

Polymer	Thermal Conductivity ($Wm^{-1}K^{-1}$)
PVDF	0.17–0.19
PTFE	0.25–0.27
PP	0.11–0.16

Table 1: Polymer Thermal Conductivity for Membrane Distillation

The following formula may be used to calculate the thermal conductivity of the PTFE membrane:

$$k_s = 4.86 \times 10^{-4} T + 0.253 \quad (7)$$

However, the thermal conductivity of MD membrane is typically taken as a volumetric average of both the conductivities combined k_s and k_g. Mathematically, it can be written as the following:

$$k_m = (1 - \varepsilon) k_s + \varepsilon k_g \quad (8)$$

After conducting various experiments, the scientist Phattaranawik suggested that the thermal conductivities can better be explained by basing them on a volumetric average of their resistances ($1/k_s$, $1/k_g$) rather than conductivities and mathematically could be written as the following [16]:

$$k_m = \left[\frac{\varepsilon}{k_g} + \frac{(1-\varepsilon)}{k_s} \right]^{-1} \quad (9)$$

We also come to figure out that the thermal conductivities for air and water vapours at standard temperature and pressure i.e., $25^{O}C$ are having the same magnitude. To further explain this fact, if we look at the thermal conductivities, they are 0.026 $Wm^{-1}K^{-1}$ for air and for water vapour it is 0.020 $Wm^{-1}K^{-1}$. this result helps us justify the assumption that component of air is present in the pores inside the membrane.

Some further recommendations in order to reduce the thermal conductivity were published by Khayet [17], in which he explained that if membranes with low thermal conductivities were used, having higher porosity and thickness, it would minimize heat loss. The publication further mentioned that the usage of composite hydrophilic/hydrophobic membrane could increase the permeability of the system. The combination nomenclature consisted of a membrane with an extremely thin layer of hydrophobic membrane coated on a hydrophilic material making up a thick membrane to stop the feed water from wetting the membrane.

- **Mean pore size and distribution inside the membrane**

The common size of membranes under usage in the industry is usually between 100nm to 1μm [18]. The permeate flux is directly proportional to the pore size of the membrane. The pore size is also helpful in determining the mass transfer through the membrane and the mean free path taken by the permeate flux through the membrane when transferring water vapour molecules. There exists a trade-off between the pore size of the membrane and the wetting of the membrane. of course, as stated previously, a larger pore size will help in obtaining a higher permeate flux, while simultaneously the membrane pore size should not allow the water from the feed to wet the membrane. Hence, as a result, the operating conditions and feed solution play an important role in determining the pore size of the membrane to be used for operations.

It is a matter of fact that the membrane does not have a uniform pore size, so there are other mechanisms than mass transfer that are being conducted simultaneously inside the membrane. The scientific community in fact on this matter is not on the same side. Khayet in his publication reported that we need to take extreme care when mean pore size is being utilized to calculate the vapour transfer coefficient instead of the pore size distribution [19]. However, in another publication it was reported that the similar vapour transfer coefficients were obtained when mean pore size and pore size distribution were both used in calculations [20].

Some of the methods that are used to examine the pore size separation parameters of the membrane include the following:

  - Scanning Electron Microscopy (SEM)
  - Atomic Force Microscopy (AFM)
  - Bubble point with gas permeation (wet and dry flow method)
  - Permeability method

2.2.3 Mechanisms involved in Direct Contact Membrane Distillation

- **Mass Transfer**

  In the following scenario, the mass flow (J) is considered to be proportional to the difference in vapour pressure across the membrane. Mathematically, it can be written as:

$$J = C_m[P_2 - P_3] \quad (10)$$

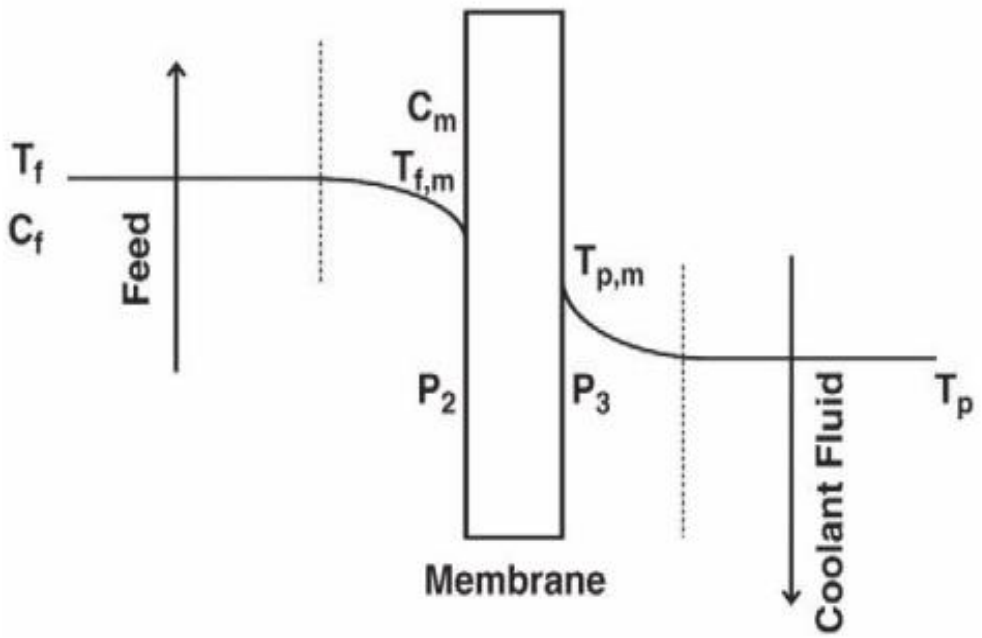

Figure 8:schematic of direct contact membrane distillation

Where in the above-mentioned equation, C_m is the membrane co-efficient, P_2 and P_3 are the membrane feed and permeate surfaces. The two values can be calculated from the Antoine equation [21]. Furthermore, the above-mentioned equation (10) can be written in the following manner by considering the temperature difference across the membrane. It is to be noted that the equation is valid for when the separation process is carried out for pure water or extremely diluted solutions, in addition the temperature difference cross the membrane should be less than or equal to 10°C [22]. Hence in mathematical form, the equation is then transformed into the following:

$$J = C_m \frac{dP}{dT}(T_{f,m} - T_{p,m}) \quad (11)$$

The pressure differential relation in the above equation can be related to temperature from the Clausius-Clapeyron equation, which is as follows:

$$\frac{dP}{dT} = [\frac{\Delta H_v}{RT^2}]P_o(T) \quad (12)$$

Here in the equation, R is the universal gas constant and ΔH_v represents the latent heat of vaporization. It is also to be noted that the Antoine equation can only be used for the representation in low concentration solutions because of the fact that it can only then be assumed that the vapor pressure is function of temperature only and not dependent on solution concentration.

There are three models for mass transport via the membrane. On the basis of these models, collisions between molecules and membrane due to mass transfer can be explained. In his publication, Zhongwei [23] suggested that the Knudsen diffusion occurs in the scenario in which the pore size is overly small. The concept is based on the idea that collisions between molecules and the membrane's interior walls are sufficient to create a mass transfer expression, and so collisions between molecules may be neglected. On the other hand, molecular diffusion is said to take place when the molecules move corresponding to each other and are influenced by concentration gradients. The last model that helps in explaining the Poiseuille model. The model is based on viscous flow, in which the gas molecules act as a continuous fluid which has its main driving force of pressure gradient [4].

If we talk about the Knudsen diffusion model, the ratio of mean free path (λ) of molecules being transported to the size of the membrane size in known as the Knudsen number (Kn). The kinetic theory of gases assumes the molecules to be hard spheres, in having a diameter d_e. the molecules are then involved in binary collisions only. One point worth mentioning is that the collision diameters of water vapour and air are approximately 2.64×10^{-10} and 3.66×10^{-10} meters respectively. The following formula can be used to help estimate the average distance travelled by molecules in order for the collisions (λ) to occur.

$$\Lambda = \frac{k_B T}{\sqrt{2}\,\pi P {d_e}^2} \quad (13)$$

Here in the equation, the variables are as follows: k_b is the Boltzmann constant, T is the absolute temperature, and P is the average pressure within the membrane pores

respectively. Al-Obaidani in his publication figured out that the mean free path value for water at 60ºC was about 0.11µm.

The Knudsen number is a good indicator in order for us to understand what kind of collisions are taking place. For example, if $k_n > 1$ or $d_p < \lambda$, also known as (Knudsen region) it means that the mean free path of water vapours molecules is larger in comparison to the membrane pore size, as a result, molecule-pore wall collisions may be more important than molecule-molecule collisions. The mass transfer is then be found out by the following equation:

$$C_{kn} = \frac{2\pi}{3}\frac{1}{RT}\left(\frac{8RT}{\pi M_w}\right)^{1/2}\frac{r^3}{\tau\delta} \quad (14)$$

Where in the equation, τ represents the membrane tortuosity, r represents the pore radius, δ represents the membrane thickness, and the M_w represents the molecular weight of water vapour respectively.

Similarly, in the second case of the $k_n < 0.01$ or $d_p > 100\ \lambda$, (Continuum Region), the vapour flux transfer through the stationary air film can then be represented by ordinary diffusion model. Ordinary molecular diffusion is helpful in figuring our mass transfer:

$$C_D = \frac{\pi}{RT}\frac{PD}{P_{air}}\frac{r^2}{\tau\delta} \quad (15)$$

Here the new variables, P_{air} represents the air pressure within the membrane pore, D represents the diffusion coefficient, and P represents the total pressure within the pore, which should be equal to the partial pressure of air and water vapour. Here the flux of water vapours than come out to be:

$$J = \frac{1}{P_{air}}\frac{\varepsilon}{\tau\delta}\frac{DPM_w}{RT}\Delta P \quad (16)$$

Where ε is the porosity of the membrane.

Here in this case, if the feed and permeate is degassed, it will result in reducing the molecular diffusion resistance, hence it shall help in the increase of membrane permeability.

Discussing the last case, in which the if $0.01 < k_n$ or $\lambda < dp < 100\ \lambda$ (called the transition region), the water vapour molecules are in constant collisions with each other, which also helps them in diffusing them through the air film. So subsequently, the mass

transfer is due to both the mechanisms of Knudsen and ordinary molecular diffusion where it can mathematically state that membrane coefficient becomes:

$$C_c = \frac{\pi}{RT}\frac{1}{\tau\delta}\left[\left(\frac{2}{3}\left(\frac{8RT}{\pi M_w}\right)^{0.5} r^3\right)^{-1} + \left(\frac{PD}{P_a} r^2\right)^{-1}\right]^{-1} \quad (17)$$

Concerning the above-mentioned models, a tremendous amount of research has been carried out already and various scientists have published their findings of the membrane distillation. For example, Lloyd and Lawson concluded that Knudsen and molecule-molecule collisions occur at the same time when the pore size is less then 0.5μm [11].

In another research, it was found out that flux for large pores could only be expressed by molecular diffusion [24]. Furthermore, Khayet was of the view that when pore size and mean free path (critical pore size) have comparable values, the Knudsen mechanism produces a larger permeate flow than the combination of Knudsen and molecular diffusion methods [17]. As a result, selecting membranes with tiny hole sizes may be preferable than membranes with high pore sizes. Similarly, the effect of pore size distribution on DCMD was investigated [20], and it was shown that for high pore sizes, the effect of pore size distribution may be ignored.

- **Heat Transfer**

It is now a well-known phenomenon that the membrane distillation is a non-isothermal procedure. The two main heat transferring mechanisms of the process are latent heat and conduction heat transfer. The following figure shows the heat transfer resistances that are faced by the system and are overcome to go ahead with the procedure.

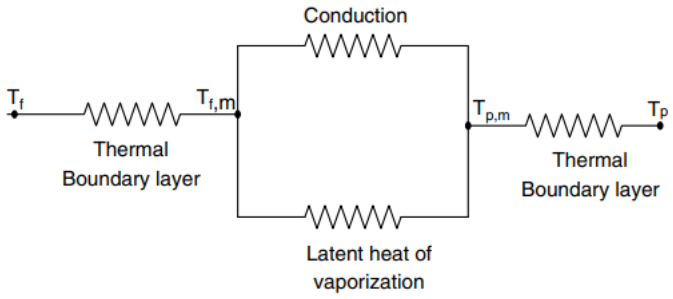

Figure 9: Resistances of heat transfer in MD system

Accordingly, the heat transfer happening in the MD system could possibly be divided into three regions [25]. The heat transfer occurring in the feed boundary layer due to convection is given by:

$$Q_f = h_f(T_f - T_{f,m}) \quad (18)$$

The second form of heat transmission happens via the membrane as a result of conduction, as well as the passage of water vapour over the membrane (latent heat of vaporization). The effect of mass transfer can be neglected in the heat transfer phenomenon in MD [26]. The heat transport across the membrane may be described numerically as:

$$Q_m = \frac{k_m}{\delta}\left(T_{f,m} - T_{p.m}\right) + J\Delta H_v \ (19)$$

Here is this equation the term $\frac{k_m}{\delta}$ can be written as:

$$h_m = \frac{k_m}{\delta} \quad (20)$$

Hence the equation 19 can be written as the following:

$$Q_m = h_m\left(T_{f,m} - T_{p.m}\right) + J\Delta H_v \ (21)$$

Here h_m is called the heat transfer coefficient of the membrane. For pure water and extremely dilute solutions with a temperature differential across the membrane of less than or equal to 10°C, the variable hm can be rewritten. From equation 11, J can be substituted in the equation 21 to transform the equation into the following expression:

$$Q_m = \frac{k_m}{\delta}\left(T_{f,m} - T_{p.m}\right) + \left[C_m \frac{dP}{dT}\left(T_{f,m} - T_{p,m}\right)\right]\Delta H_v \ (22)$$

$$Q_m = \left[\frac{k_m}{\delta} + \left(C_m \frac{dP}{dT}\right)\Delta H_v\right]\left(T_{f,m} - T_{p,m}\right) \ (23)$$

$$Q_m = h_m(T_{f,m} - T_{p,m}) \quad (24)$$

If the system is assumed to have a non-linear heat transfer in the x-direction, the conductive heat transfer Q_m can be expressed from the following [27].

$$Q_m = -k_m \frac{dT}{dx} + J\Delta H_v \ (25)$$

If we now consider the permeate side of the membrane, the convection heat transfer could be characterized by the following equation:

$$Q_P = h_p(T_{p,m} - T_P) \text{ (26)}$$

If the system is at a steady state, we can then state that the overall heat transfer flux can be represented by the following equation:

$$Q = Q_f = Q_m = Q_p \text{ (27)}$$

Putting the values in of heat transfers, we obtain the following equation:

$$h_f\left(T_f - T_{,fm}\right) = \frac{k_m}{\delta}\left(T_{f,m} - T_{p.m}\right) + J\Delta H_v = h_p(T_{p,m} - T_P) \text{ (28)}$$

$$Q = U(T_f - T_p) \text{ (29)}$$

Here in equation 29, U is the overall heat transfer coefficient of the system. Heat conduction can be neglected in the case of non-sported thin membranes and high operating temperatures. The temperature of both sides of the membrane's surface cannot be established experimentally or directly. To estimate these temperatures, a mathematical iterative model has been developed [28]. The temperatures can be found iteratively from the following equations:

$$T_{f,m} = T_f - \frac{J\Delta H_v + \frac{k_m(T_{f,m} - T_{p,m})}{\delta_m}}{h_f} \text{ (30)}$$

$$T_{p,m} = T_p - \frac{J\Delta H_v + \frac{k_m\left(T_{f,m} - T_{p,m}\right)}{\delta_m}}{h_p} \text{ (31)}$$

Here the latent heat of vaporization ΔH_v can be calculated ate average membrane temperature. Some research papers also cite this value as a logarithmic average of the membrane temperature [29]. For pure water and extremely diluted solution, the surface membrane temperature in terms of temperature polarisation coefficient, ψ, can be written as [30]:

$$T_{f,m} - T_{p,m} = \frac{1}{1 + \frac{H}{h_f} + \frac{H}{h_p}}\left(T_f - T_p\right) = \psi(T_f - T_p) \text{ (32)}$$

Where keep in mind that the value h_m for pure water and extremely diluted solutions is the following:

$$\frac{k_m}{\delta} + \left(C_m \frac{dP}{dT}\right) \Delta H_v \quad (33)$$

In another research, Lloyd and Lawson while working on diluted solutions in membrane distillation, also pointed out that the value for the difference of membrane feed and permeate side temperatures ($T_{f,m} - T_{p.m}$) does not exceed 0.1°C when the incoming flux is at a low level. While the value does not exceed 0.5°C when the flux of the incoming vapours is high [11]. The iterative procedure to calculate the unknown terms of temperature of membrane feed and permeate side, along with the heat transfer coefficients of the feed and permeate was applied on MATLAB with the experimental data inserted. The data and procedure are discussed in the methodology section of the thesis. The data was obtained from the university of Aalborg and corresponds to the water quality at the demo site located in Eilat in Israel.

2.2.4 Polarization of Temperature and Concentration

There exists a phenomenon of temperature polarization in the membrane distillation mechanism because of the fact that the vaporization occurs on the hot side of the membrane and condensation occurs on the permeate side. Thermal boundary layers form on both sides of the membrane as a result of this. Temperature Polarization refers to the temperature differential between the bulk feed temperature and the liquid-vapour interface. The following is a mathematical definition of the term:

$$\psi = \frac{T_{m,f} - T_{m,p}}{T_f - T_p} \quad (34)$$

The influence of the heat transfer boundary layer on the system's overall heat transfer resistance is measured using temperature polarization. The following figure represents the effect of temperature polarization in membrane distillation:

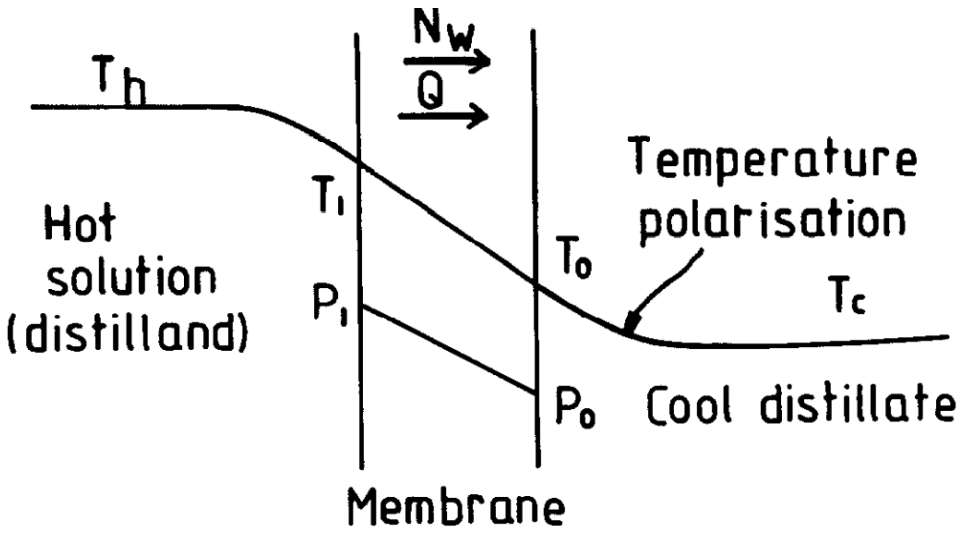

Figure 10: Membrane Distillation Temperature Profile

The term can be interpreted in the following way. If the thermal boundary layer is decreased, the temperature difference of the liquid-vapour interface and the bulk feed temperature comes close to each other, which makes the temperature polarization coefficient ψ approach unity. On the other hand, if the coefficient ψ has a value close to 0, it means that the polarization is of significant value and the two temperatures are quite far apart. Hence the system is now controlled by a large boundary layer resistance [31].

On the other hand, when we're talking about the concentration polarization coefficient Φ, the coefficient describes the increase of the solute intensity on the surface of the membrane (c_m) to the bulk concentration (c_f). Mathematically, we can write the following formula for the concentration coefficient:

$$\Phi = \frac{c_m}{c_f} \quad (35)$$

The following relationship has been given in the equation in order to approximate the accurate value of the concentration of solute (mole fraction) on the membrane surface. [32]:

$$c_m = c_f \exp\left(\frac{j}{\rho k}\right) \quad (36)$$

Where in the above-mentioned equation, $\rho \; and \; k$ are liquid density and mass transfer coefficient respectively. There is substantial evidence of the impact of high concentration on mass transfer coefficient and distillation flux, according to studies. The viscosity of the feed, its density, the solute diffusion coefficient, and convective heat transfer are all effects of concentration and temperature. The studies also conclude that the salt accumulates on the

surface of the membrane and during the process of desalination, which causes a diffusive flow in the backward direction towards the feed solution [27].

2.2.5 Operating Parameters for a Membrane Distillation system

This section includes the effect and influence of feed temperature, concentration, and air gap on the membrane distillation system. A detailed discussion is presented below:

- **Temperature of the Bulk Feed**

  The following table taken from a comprehensive review about membrane distillation reflects the effect of feed temperature on the distilled flux. The table shows a strong influence of the feed temperature on membranes made of different materials and tested with various saline solutions [4]. The Antione equation predicts that the vapour pressure has a directly proportional relation with the temperature, and it increases exponentially as the temperature increases. Therefore, it can also be stated that the operating temperature has an exponential effect on the permeate flux as well [33]. When the difference of temperature remains constant between the hot and cold fluids, there is a rise in the permeate flux due to an increase in the hot fluid temperature, implying that the permeate flux is more dependent on the hot fluid temperature [34]. It was also pointed out that the if the temperature gradient was to be increased between the surfaces of the membrane, the phenomenon will affect the concentration coefficient positively, which will then lead to an increase of flux [35].

MD TYPE	MEMBRANE TYPE	PORE SIZE (MM)	SOLUTION	FEED VELOCITY (M/S)	T_F (^{O}C)	PERMEATE (KG/M^{2}H)
AGMD	PVDF	0.45	Artificial Seawater	5.5 l/min	40-70	≈1-7
DCMD	PVDF	0.22	Pure water	0.1	40-70	≈3.6-16.2
DCMD	PTFE	0.2	NaCl (2mol/l)	16 cm^3/s	17.5-31	≈2.88-25.2
DCMD	PTFE	0.2	Pure Water	-	40-70	≈5.8-18.7
DCMD	PVDF	0.4	Sugar	0.45	61-81	≈18-38
DCMD	PVDF	0.4	Pure Water NaCl (24.6 wt%)	0.145 0.145	36-66 43-68	≈5.4-36 ≈6.1-28.8
VND	3MC	0.51	Pure water	-	30-75	≈0.8-8.8 mol/m^{2}s
DCMD	PVDF	0.22	Pure water	0.23	40-70	7-33 l/m^{2}h
SGMD	PTFE	0.45	Pure water	0.15	40-70	≈4.3-16.2
DCMD	PVDF	0.11	Orange juice	2.5 kg/min	25-45	30 × 10^3 – 108 ×103
DCMD	PTFE	0.2	NaCl (5%)	3.3 l/min	5-45	1-42
AGMD	PTFE	0.2	NaCl (3%)	3.3 l/min	5-45	0.5-6

Table 2: temperature effect on Permeate Flux

As far as the coolant temperature in concerned, there is a perceptible change in the permeate flux when the temperature of the cold side decreases. But there are also studies that depict that the cold side temperature effect can be neglected on permeate flux as compared to hot side, due to the fact that the vapour pressure change is negligible at low temperatures [36].

- **The solution concentration**

When feed concentration rises, the flux product decreases significantly due to decreased vapour pressure and increased temperature polarization [37]. Furthermore, investigations have revealed that the decline in product flow is proportional to time. The effect of acid concentration on permeate flux was investigated. They discovered that when the acid concentration rises, the permeate decreases [38]. A study also concluded that the permeate flow drops marginally with increasing feed concentration, according to the findings. When the feed (NaCl) concentration was raised from 0 to 2 Molar, the permeate flow was reduced by around 12% [39]. The decrease in permeate flow can be attributed to a drop in vapour pressure. When the concentration of NaCl rises, Lawson and Lloyd [11] looked into why product flux decreases. They discovered three causes for this decrease: 1) water activity,

which is a function of temperature, drops as concentration rises; 2) The mass transfer coefficient of the boundary layer at the feed side reduces as the impact of concentration polarization increases, and 3) the heat transfer coefficient of the boundary layer drops as the surface membrane temperature lowers. As a result, the feed's vapour pressure drops, resulting in decreased MD performance. For salt solutions, the effect of density on flux generation is also significant. Garcia et al.[9] investigated three aqueous solutions of methanol, ethanol, and isopropanol at various concentrations. They discovered that the quantity of flux is substantially linked to the type of alcohol consumed. Because isopropanol has the highest vapour pressure, its solution has the highest flux, following the same principal, methanol solution has the lowest. Yun [27] reported on the effect of high concentrations, such as in NaCl solutions, finding that the permeate flux varies with time (see Table 3) and that calculating the permeate flux using existing models is problematic.

MD TYPE	MEMBRANE TYPE	PORE SIZE (MM)	SOLUTION	CONCENTRATION G/L	T_F (^OC)	PERMEATE (KG/M^2H)
AGMD	PVDF	0.22	Methanol/Water	≈ 30-200	50	≈3.9-4.6
			Ethanol/Water	≈ 30-150		≈ 3.95-4.9
			Isopropanol/Water	≈ 10-95		≈4.0-5.0
DCMD	PTFE	0.2	NaCl	0-116.8	31	≈32.4-25.2
DCMD	PVDF	0.4	NaCl	0-5290	81	≈44-63
DCMD	PVDF	0.22	NaCl	0-24.6 wt%	68	≈36-28.8
AGMD	PTFE	0.22	HNO_3	2-6M	80	≈ 0.9-2.1 l/m^2h
VMD	PP	0.2	NaCl	100-300	55	10.7-7

Table 3: relation of permeate flux with concentration

- **Rate of Recirculation**

The effect of the recirculation rate is summarized in table 4. Increasing the recirculation rate lowers boundary layer resistance and improves heat transfer coefficient. As a result, larger flux levels are possible [15]. A study concluded that the permeate flux is directly proportional to the increase of volumetric flow rate. The fluid velocity rises as the volumetric flow rate increases, causing the convective heat transfer coefficient to develop and the thickness of the thermal boundary layer to decrease. Consequently, the polarity impact of

temperature decreases. When it comes to the cold side flow rate, research show that increasing the cold side flow rate has no influence on the permeate flux. [40].

MD TYPE	MEMBRANE TYPE	PORE SIZE (MM)	SOLUTION	T_F (^OC)	FLOWRATE (M/S)	J (KG/M^2H)
SGMD	TF200 TF450	0.2 0.45	NaCl (1M)	50	0.07-0.21	≈ 3.24-3.96 ≈5.4-5.76
DCMD	PVDF	0.22	NaCl (35 g/l)	60	1.85-2.78	31-38
AGMD	PVDF	0.45	Artificial Seawater	60	1-5.7 l/min	≈2.7
DCMD	PTFE	0.2	Sucrose (40 wt%)	39	5-16 cm^3/s	5.7-9.0
DCMD	PVDF	0.4	Sugar (30 wt%)	81	0.45-0.9	≈38-55
DCMD	PVDF	0.22	NaCl (17.7 wt%)	68	0.056-0.33	≈25.9-29.5
VMD	3MC	0.51	Pure Water	74	37-63 cm^3/s	≈6.4-8.7 mol/m^2S
DCMD	PVDF	0.22	Pure Water	50	1.8-2.3	≈18-20 l/m^2h
VMD	PTFE	0.2	Acetone (5 wt%)	30	0.1-2.6 l/min	12.6-21.6
VMD	PP	0.2	NaCl (300 g/l)	55	0.015-0.03 l/s	7-9.1

Table 4: Relation between recirculation rate and permeate flux

- **Type of Membrane**

The porosity of a membrane affects its permeation flow, which is inversely proportional to its thickness and tortuosity [41]. It was observed in studies that the permeate flux of the membrane is directly proportional to the pore size. Such that for a larger pore size, the flux obtained was larger in comparison to smaller pores. Furthermore, it was observed that as compared to the same membrane hole size with support, a membrane without support achieves higher flow. In a case study, it was found that low thermal conductivity material (unsupported membrane) should be utilized for an efficient MD process [33].

2.3 Review of Comparative Technologies

In this section, a brief literature review of the technologies compared with membrane distillation is discussed. The technologies that are being discussed are basically nanofiltration and sterilization unit, specifically the HiNaPEF generator that is also installed at the demo site 2 in Eilat, Israel. The two technologies that will be discussed in this section will then be used as a comparison to check whether the membrane distillation technology is better in terms of efficiency or maybe the compared technologies perform better. Following is a succinct explanation of the literature that exists about the technologies.

2.3.1 Nanofiltration

Nanofiltration (NF) membranes have gone a long way since their discovery in the late 1980s. The pore size of NF membranes is 1 nm, which equates to a molecular weight cut-off (MWCO) of 300–500 Da, and they have features that are halfway between ultrafiltration (UF) and reverse osmosis (RO) [42]. Due to the dissociation of surface functional groups or the adsorption of charge solutes, NF membranes in contact with aqueous solution are also mildly charged. In the presence of a feed solution, polymeric NF membranes, for example, include ionizable groups such as carboxylic and sulfonic acid groups, resulting in a charged surface. NF membranes, like RO membranes, are effective at separating inorganic ions and small organic compounds. NF membranes feature a lower monovalent ion rejection, a larger divalent ion rejection, and a higher flow than RO membranes. Because of these qualities, water and wastewater treatment, pharmaceutical and biotechnology, and food engineering are just a few of the specialist uses for NF.

Mechanisms for separations used in Nano-filtration

The NF process is dependent on the micro-hydrodynamic and interfacial processes that occur at the membrane surface and within the membrane nanopores. NF membrane rejection can be caused by a mixture of steric, Donnan, dielectric, and transport mechanisms. The steric mechanism (size-based exclusion) is used to transport neutral solutes and has been extensively proven by several investigations of UF membranes [43]. The equilibria and membrane potential

interactions between a charged species and the charged membrane interface are described by the standard Donnan effect [44]. The membrane charges up due to the alienation of ionizable groups at the membrane surface and also inside the membrane pore structure. [45].

NF membranes have a poor ion exchange capacity, and ions from the contacting solution may adsorb to the membrane surface, resulting in a small charge modification. [46]. As a result of the aforementioned events, electrostatic repulsion or attraction occurs based on the ion valency and charge of the membrane, which might be variable depending on the specified ionic environment. Dielectric exclusion is a far less well-understood phenomenon, with two competing hypotheses as to the actual nature of the interaction.

Solutes traveling in free solution are dragged by the solvent flowing through the limited pore structure. The local environment has a significant impact on solute transportation in this limited region, and solute transport is believed to be hampered. Hindered transport has a convective and diffusive component, both of which contribute to the overall transport effect. Because the dimensions of the NF active layer are on the order of atomic length scales, combined with current measurement technology limitations, detailed knowledge of the physical structure and electrical properties of real NF membranes has been slow to develop, leading to uncertainty and heated debate about the true nature of the separation mechanisms.

Nanomaterials for Nano-filtration Membranes

Nanoparticles (NPs) have recently attracted a lot of attention due to their unique photoemission, antibacterial, and catalytic capabilities. NPs integrated membranes have gained a lot of interest because of their capacity to improve membrane permeability, mechanical properties, hydrophilicity, and selectivity in particular instances. The most often utilized NPs in NF membrane manufacture are titanium dioxide (TiO2), silica, silver, and zinc oxide (ZnO) [42].

Nanoparticles (NPs) have recently attracted a lot of attention due to their unique photoemission, antibacterial, and catalytic capabilities. Because of their ability to boost membrane permeability, mechanical characteristics, hydrophilicity, and selectivity in some situations, NPs integrated membranes have gotten a lot of attention. Titanium dioxide (TiO2), silica, silver, and zinc oxide are the most often used NPs in NF membrane manufacturing (ZnO) [47]. Because of its remarkable bio-catalytic performance, the functionalization of TiO2 with immobilized laccase has also gotten a lot of interest. Because of the covalent interaction between the

mounted enzyme and TiO2 membranes, the laccase enzyme's stability and activity might be increased. The membrane was said to have improved BPA removal efficiency, making it a viable alternative to the traditional wastewater treatment technique. Aside from using a single type of NP, combining two types of NPs can boost membrane performance significantly. A novel PES nanocomposite membrane was created using polyaniline and iron (II, III) oxide [PANI/Fe3O4] NPs produced by in situ chemical oxidative polymerization. The key features of PANI and Fe3O4, which might aid in the removal of heavy metals and natural organic matter, were demonstrated to significantly improve Cu(II) removal from water [48]. Functionalized multi-walled carbon nanotubes [49], halloysite nanotubes, and electro spun nanofiber were among the other fascinating nanomaterials used in membrane construction. By combining all of these innovative nanomaterials into membrane manufacture, the objective of significantly improving the NF membrane and other types of membranes can be achieved in the near future.

2.3.2 Pulses Electric Field application to water treatment

The pulsed electric filed application to water treatment system is relatively a new technology and which is still under review. Many experiments and studies are being conducted in order to check out the applications, pros, and cons of the technology. Whether it can be a sustainable alternative to any existing machinery that might be less efficient in comparison. The technology is not only limited to water treatment but can be also effective for cleaning different surfaces and equipment effectively. For example, the technology can be used to clean and reuse surgical equipment. The pulsed electric field can open a vast universe of many applications. One of these is cancer therapy using an ultra-short pulse high electric field [50]. The usage of the technology in the demo site in Eilat is to sterilize the water that is going out of the facility back and into the sea, maybe also used for other purposes.

Mechanism for Pulsed Electric field Water treatment

In pulsed electric field pasteurization, a liquid or semiliquid product is placed between two electrodes and a pulsed electric field is applied (PEF). A high-voltage electric field is used to subject a fluid pumped between two electrodes to repeated short pulses. The result is to increase the number of holes in plant and animal cell membranes, causing the cells to lyse. However, no significant temperature increase is required to destroy germs. Bacterial, yeast, and fungal cells

would require >30 000 V to die, although it is yet unknown if viruses or spores can be inactivated. The creation of large, permanent holes in cellular tissues aids in the improvement of juice output, the rise of functional component concentrations, and the enhancement of dried produce properties. PEF is most commonly utilized in refrigerated or ambient items, and because it is only administered for 1 second, it does not cause the product to heat up. It provides nutritional advantages over more standard thermal methods that damage heat-sensitive nutrients because of this. However, most enzymes are unaffected by PEF, which might induce degradation in juice under ambient circumstances, necessitating the refrigeration of treated items to maintain their organoleptic quality. PEF technology has been used to successfully pasteurize foods such as juices, milk, yogurt, soups, and liquid eggs. [51].

3. Methodology adapted and backdrop of demo site

3.1 Background and Demo site explanation

The framework will be discussed in this chapter, along with calculations carried out using the data obtained from the project partners involved. The information and values involved in the calculations are the property of the partners involved and are listed after consulting them and according to their consent. The calculations also involve a few assumptions due to the fact the world is going through a pandemic which has caused many delays and unforced closures to many experiments and studies. The experimentation and analysis were conducted in special collaboration with IRIS s.r.l and the energy department DENERG (Dipartimento Energia "Galileo Ferraris") of Politecnico Di Torino.

The demo site located in Eilat; Israel is the main focus of the calculations. As mentioned above, the demo site includes a fishpond, to put in simple words, and the main goal is to prove the feasibility of recycling the water of Eilat land based marine aquaculture in a cost effective and environmentally friendly way. The IOLR National Centre of Mariculture in Eilat is a world leader in mariculture, a new aquaculture branch that uses both marine and brackish water. Growing demand for fish products, land and water scarcity, and environmental concerns have caused aquaculture to migrate away from its traditional technique and location and toward the use of Recirculating Aquaculture Systems (RAS). The key issues in RAS are preserving water quality and, in particular, treating nitrogen build-up from protein metabolism so that water may be reused in a nearly closed loop.

The wastewater produced by the fish culture system is 250 cubic meters per hour. The RAS uses biofilters to cleanse water, primarily for the two-step oxidation of ammonia, which is particularly harmful to fish even at low quantities. In contrast, nitrate, which is formed when ammonia is oxidized, is less hazardous and may build in the fish-growing system to rather high levels, allowing for a significant reduction in the rate of external water exchange. Such nitrate-rich wastewaters, which are also high in phosphorus, cannot, however, be dumped into the marine or natural environment (might cause eutrophication).

Nonetheless, neither for marine RAS nor for sea water desalination facilities, efficient and cost-effective methods for nitrate removal from marine wastewater have been well established. As a result, rather than dilution, brine and effluent from desalination facilities and land-based fish farming RAS are dumped directly into the sea. Another difficulty with recirculation of aquaculture systems is the requirement to disinfect the effluent, which adds operating costs and perhaps reduces output profitability. Reducing the effluent flow rate (by lowering the external water exchange rate) would lower disinfection expenses; but, a very low water exchange rate would result in the build-up of fine size suspended particles (less than 15 m), which would degrade internal water quality and hinder fish development.

Other obstacles to complete water recirculation in the RAS include high salinity and BOD levels, which can quickly grow in totally closed recirculated marine fish culture systems. Encouraged by the growing desire to increase aquaculture production through multiple RAS facilities, one of the major objectives of the proposed project is to evaluate and scale up efficient technological solutions for marine wastewater treatment, recycling, and reuse, thereby accelerating the sector's successful development.

3.2 Opportunities for technological exploration at the demo site

Implementing a unique marine water denitrification reactor in combination with a macro-algae polishing treatment in Eilat can open up the possibility of recovering nutrients from wastewater generated by the fish culture system or the desalination plant: algal biomass has the potential to be used as high-protein fodder enhancements for aquaculture (and/or livestock such as chickens, cows, and pigs), neatly closing the circle of a self-feeding system. The similar principle may be applied to other scenarios in which nutrient removal is necessary prior to wastewater release, with algal biomass serving as a potential biofuel matrix. Scaling up the

facility and incorporating disinfection, salinity control, and denitrification technologies would allow for close to 100 percent closed loop reuse of (sea)water, with the evaporated component of the water being restored. Furthermore, the wastewater flow is of a volume adequate for testing a small-scale desalination plant to provide water suitable for irrigation (SAR maximum medium value: 5 (Mmol/L)0.5).

3.3 Water treatment module (SALTECH) installed at the Demo site

The following table provides a brief overview of the water quality found at the demo site in Eilat. The major issues and critical parameters are highlighted.

Parameter	*Unit*	*Output*	*Input Requirements*
Salinity	ppt or gr/l	40	14-40
Total dissolved solids	mg/l	40,000	14,000-40,000
Water Temperature	Celsius	20-30	18-30
Nitrate	mgN/l	20-100	Flexible
pH		7-8	7-8
Total ammonia Nitrogen	mgn/l	2-8	<1
Total P	mgP/l	1-20	<1
Total suspended particles	TSS	20-80	<5
BOD_5	mg/l	10-40	<10
Alkalinity	mg/l C_aCO_3	75-150	-Flexible

Table 5: values of wastewater from saltwater aquaculture pond in Eilat

Three technologies are imagined as being capable of achieving this goal: 1- biological mixed treatment (BMT) for denitrification, the pilot scale denitrification treatment that will be executed in the RAS setup will be sponsored by Israeli state sources, with matching funding from a public and private source. A polishing algae treatment will be applied during Project demonstration operations, based on the utilization of macro-algae assimilation for nitrate removal from marine effluent. This method needs huge surface areas for algal growth but provides commercially useful algae as a by-product:

- desalination methods with low energy usage for reducing salty content.

- AOP technology for organic molecule breakdown and disinfection (HiNaPEF for sterilization and Advanced Adsorption for DOC abatement). SALTECH, a pilot module that incorporates these technologies, will be shown to recycle 20 cubic meters of water every day.

Aside from water recycling, the Project team plans to look into the possibilities of treating and reusing a portion of the wastewater for irrigation. The wastewater must be desalinated before it can be used for irrigation. Because solar energy may be employed as a source of the thermal energy necessary for the distillation process, Molecular Separation Membrane (MSM) technology is particularly ideal for this purpose given the climate conditions in Eilat. In terms of costs and risk, 20 m^3/day is a realistic scale given the technology's low TRL starting point.

Furthermore, in line with the Project's notion of tiny water loops, this size is not far off from the real-world use of such desalination plants, namely, serving a small community of people who will be able to get their water straight from the sea. Validating such technology, on the other hand, would have a major effect as a small-scale, renewable-energy-fuelled alternative to commercially accessible desalination equipment.

3.4 Adapted Methodology for membrane distillation calculations

The methodology adapted for calculations for the membrane distillation efficiency calculations cater for finding out different parameters for concluding the overall working efficiency of the device. These parameters explain some of the important characteristics which help in figuring out if the system as well as the molecular separation membrane are working accurately.

The system has already been discussed in detail in the literature review, here in this section, the discussion will focus over adapted methodology which enables for the calculation of the parameters which will be discussed below.

The system under investigation on the demo site is the Direct Contact Membrane distillation system. To provide a brief overview of the system, it is the type of membrane distillation which is thought of as the oldest and extensively used method. The procedure involves the liquid phase to be in touch mutually on the sides of membrane as shown in figure [52].

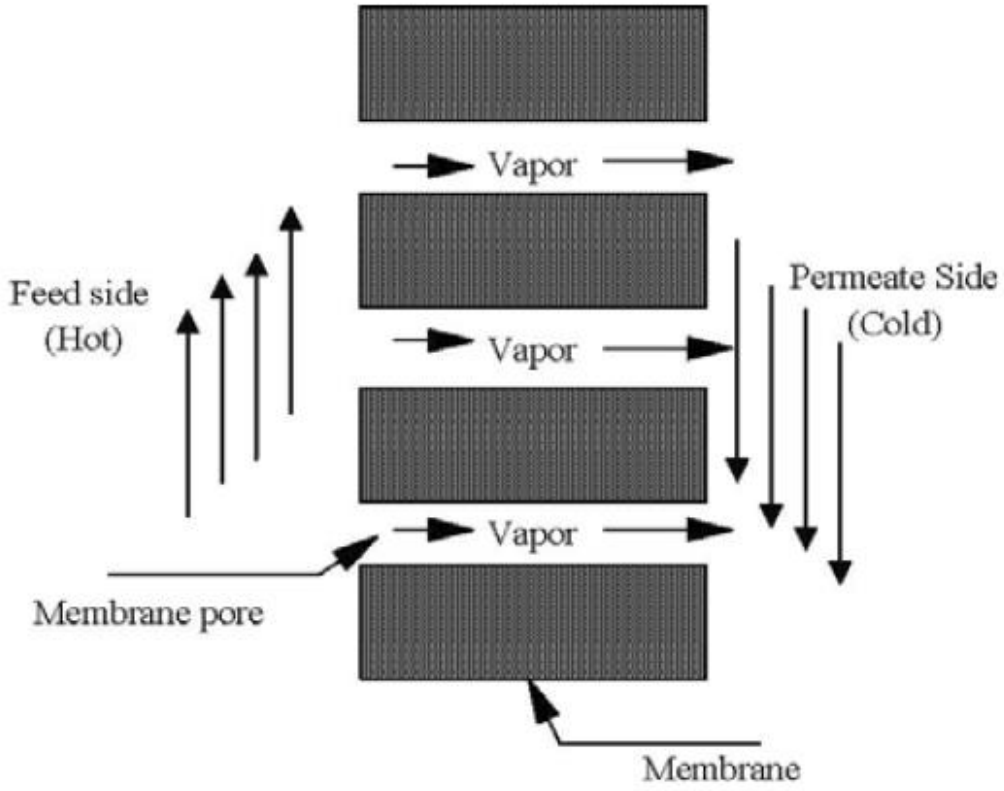

Figure 11: Direct contact membrane distillation schematic[52]

The thickness of the membrane restricts the vapour diffusion channel, lowering mass and heat transfer resistances. The prevention of condensation within the pores takes place when the right membrane material is used along with the adjustment of temperature differential across the system. In DCMD, transfer of heat and mass happen at the same time, resulting in a complicated heat transfer process. As a result, the mass transfer rate or permeate flow affects the heat flux and heat transfer coefficients on both the feed and permeate sides.

Heat loses play an important role in the overall procedure. Rather they are categorised as one of the drawbacks of the procedure. This heat loss leads to a temperature difference between the membrane/interface temperature and the bulk temperature. The driving force for water vapour migration through the membrane pores is a temperature difference between the feed/membrane interface temperature (T_{mf}) and the permeate/membrane interface temperature (T_{mp}). The temperature differential produces the effect of reduction of the driving force, which is the difference between the bulk (T_{bf}) and permeate (T_{bp}) temperature of the feed.

As discussed previously, the phenomenon mentioned above is known as temperature polarization. This results in a coefficient known as the temperature polarization coefficient, which is the ratio of the real and predicted driving forces. Mathematically, it can be written as the following:

$$TPC = \frac{T_{mf} - T_{mp}}{T_{bf} - T_{bp}} \quad (37)$$

Because determining membrane/interface temperatures experimentally is exceedingly difficult, these temperatures are usually measured using a heat balance that compares them to bulk temperatures [53]. For the heat balance to be solved for the membrane interface temperatures, it is compulsory to first measure the heat transfer coefficients in the neighbouring boundary layers.

In general, these are evaluated using empirical correlations in order for the Nusselt number to be evaluated. Furthermore, The MD configuration does not always allow for the evaluation of the flow's momentum characteristics, for example, the hydraulic diameter of the flow channel or the velocity of the flow, which augments the complications and tasks in estimating the Reynolds number (Re), which is virtually constantly present in the observed correlations used to determine the heat transfer coefficients of the boundary layers. Hence numerical methods and experimental techniques are employed for the determination of parameters such as heat transfer coefficients etc. that are required in order to proceed further with the system evaluation of membrane distillation procedures.

The transfer of heat taking place in the membrane distillation system can be divided into 3 regions. The first can be labelled as the convectional transfer of heat which is happening in the boundary layer corresponding to the feed section, and the transfer of heat taking place due to transfer of mass through the feed thermal boundary layer, we call them $Q_{f,conv}$ and $Q_{f,M.T}$ respectively. The second process combines conductive heat transfer across the membrane with mass transfer caused by water vapour migration across the membrane. Let us call them $Q_{m,cond}$ and $Q_{m,M.T}$ respectively. The last heat transfer mechanism taking place is the combination of convectional heat transfer in the permeate boundary layer and mass transfer through the permeate thermal boundary layer. Let us call them $Q_{p,conv}$ and $Q_{p,M.T}$ respectively. This transfer of heat can be better understood by the following diagram on the next page which depicts and electrical analogy of heat transfer mechanism.

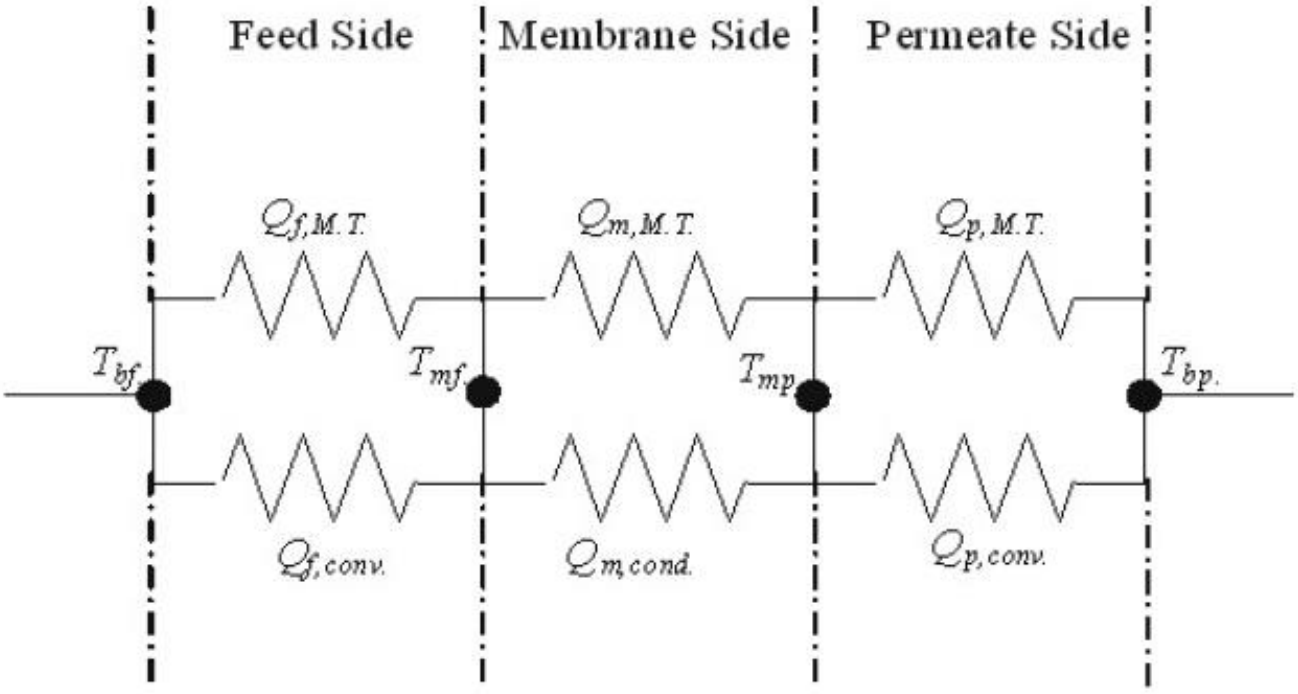

Figure 12: Electrical circuit analogy of heat transfer resistances in DCMD [52]

All the transfer of heat procedures can then be mathematically stated by the following equations.

- Heat transmission in the thermal boundary layer of the feed solution:

$$Q_f = Q_{f,conv} + Q_{f,M.T} = h_f(T_{bf} - T_{mf}) + J_w H_{L,f}(\frac{T_{bf}+T_{mf}}{2}) \quad (38)$$

- Heat transfer through the membrane:

$$Q_m = Q_{m,cond} + Q_{m,M.T} = h_m(T_{mf} + T_{mp}) + J_w H_v \quad (39)$$

- The permeate thermal barrier layer allows heat to pass through:

$$Q_p = Q_{p,conv} + Q_{p,M.T} = h_p(T_{mp} - T_{bp}) + J_w H_{L,p}(\frac{T_{mp}+T_{bp}}{2}) \quad (40)$$

The variables used in the above equations are defined as following:

1. The heat transfer coefficient of the feed boundary layer is h_f.

2. The heat transfer coefficient of the permeate boundary layer is h_p.

3. J_w is the permeate flux.

4. The enthalpy of water vapour is Hv.

5. The feed solution enthalpy is $H_{l,f.,}$ which can be mathematically calculated at the median temperature of feed solution and feed/membrane boundary. Such that at $\left(\frac{T_{bf}+T_{mf}}{2}\right)$.

6. $H_{l,p}$ is the enthalpy of the permeate solution, which is mathematically calculated at the average temperature of permeate solution and permeate/membrane interface. Such that at $\left(\frac{T_{bp}+T_{mp}}{2}\right)$.

7. Whereas the value for T_{bf} can be calculated as the average temperature of the incoming and outgoing feed. Mathematically, we can use the following corelation.

$$T_{bf} = \frac{T_{bf,in}+T_{bf,out}}{2} \quad (41)$$

8. Whereas the value for T_{bp} can be calculated as the average temperature of the incoming and outgoing permeate flow. Mathematically, we can use the following corelation.

$$T_{bp} = \frac{T_{bp,in}+T_{bp,out}}{2} \quad (42)$$

9. In the above-mentioned equations, the variables T_{mf} and T_{mp} are temperatures corresponding to the interface of membrane and feed and membrane and permeate respectively.

10. The hydrophobic membrane's heat transfer coefficient is h_m. The value for the heat transfer coefficient can be calculated by the following formula:

$$h_m = \frac{k_g\varepsilon + k_m(1-\varepsilon)}{\delta} \quad (43)$$

11. The variables in the equation 43 are kg, which is the thermal conductivity of the air trapped inside the membrane, km, which is the thermal conductivity of the hydrophobic membrane polymer, δ is the thickness of the hydrophobic membrane and ε is the porosity of the hydrophobic membrane.

After the above-mentioned parameters are figured out, some are found via thermodynamic tables and some calculated, the evaporation efficiency can be calculated. The ratio of heat transferred due to water vapour relocation through membrane openings to total heat transmitted through the membrane pores is named evaporation efficiency, or EE [54]. Arithmetically, the evaporation efficiency can be written as:

$$EE = \frac{Q_{m,M.T}}{Q_{m,M.T} + Q_{m,cond}} \quad (44)$$

$$EE = \frac{J_w H_v}{J_w H_v + h_m(T_{mf} - T_{mp})} \quad (45)$$

Khayet in his research has shown in detail the heat transfer mechanisms in membrane distillation. The research shows that the above mentioned all six heat transfer variables do not equally take part in the heat transfer. Rather some transfer values super cede and overshadow the other values to such extent that they can be neglected without having major differences in values which helps is easing up the calculations for further parameters as well. To further explain the contributions, Khayet performed calculations in which he depicted some contributions can easily be neglected.

During the procedure, the Q values were evaluated by balance of energies, whereas the $Q_{f,M.T}$ and $Q_{p,M.T}$ were evaluated by using the average bulk and permeate feed temperatures rather

than the average of the bulk/membrane surface temperatures [52]. The reason behind this adaptation was the assumption that there will be insignificant change in the liquid enthalpies as the temperature change will be minor. The following table shows the values of the above-mentioned parameters along with temperatures that were obtained.

Tbf *(°C)*	Tbp *(°C)*	Q*(10^3 W/m^2)*	$Q_{f,M.T}$ *(W/m2)*	$Q_{p,M.T}$ *(W/m2)*	*$(Q_{f,M.T}/Q)*100$*	*$(Q_{p,M.T}/Q)*100$*
34.5	11.5	17.763	256.7	90.02	1.45%	0.51%
44.85	13.65	26.778	566.1	178.33	2.11%	0.67%
50.5	15.28	34.176	1093.4	340.98	3.2%	1.0%
55.93	18.28	45.1801	1976.8	645.34	4.3%	1.43%

Table 6: Mass transfer contribution to the overall heat flux at different temperatures [52]

As depicted in the table 5, when the temperature is increased, the percentages of $Q_{f,M.T}$ and $Q_{p,M.T}$ increase, but the former increases more as compared to the latter depicting the higher mass flux in the at higher feed temperatures. But looking at the contribution of both the heat values in question to the overall heat value, the values presented show a negligible contribution. Hence, as a result, mass transfer effect on the total heat transfer in the feed and permeate boundary layer can be in fact neglected.

To depict the heat resistances once again in an electrical analogy model, the following figure depicts the effect of only significant heat transfers after neglecting the minor transfers.

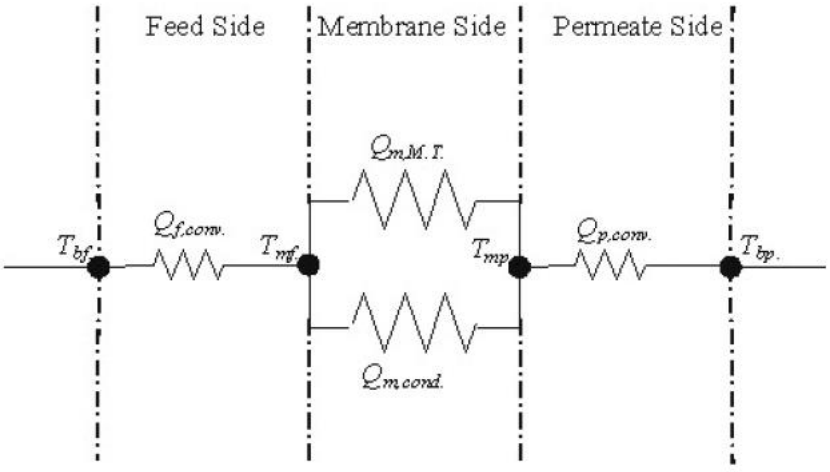

Figure 13: modified electrical analogy for heat transfer[52]

The controlling mechanism for heat transmission in the bulk and permeate feed boundary layers, according to the explanation above, is convectional heat transfer. Moreover, it can also be proved that the vapour enthalpy H_v, is practically the same as latent heat of vaporization ΔHv. Hence, we can now make amendments in the above-mentioned equations 38-40. Based on the above estimates, we obtain the following equations:

$$Q_f = h_f(T_{bf} - T_{mf}) \text{ (46)}$$

$$Q_m = h_m\left(T_{mf} - T_{mp}\right) + J_w \Delta H_v \text{ (47)}$$

$$Q_p = h_p(T_{mp} - T_{bp}) \text{ (48)}$$

At the steady state, the DCMD's overall heat flux can be given by Q, and mathematically it is equal to:

$$Q_f = Q_m = Q_p = Q \text{ (49)}$$

If we combine the above 46-48 equations, we can obtain the following value for the heat flux:

$$Q = \left[\frac{1}{h_f} + \frac{1}{h_{,m} + \frac{J_w \Delta H_v}{T_{mf} - T_{mp}}} + \frac{1}{h_p}\right]^{-1} (T_{bf} - T_{bp}) \text{ (50)}$$

Taking from the equation (50), we can then now determine the overall heat transfer coefficient (U) for the DCMD process:

$$U = \left[\frac{1}{h_f} + \frac{1}{h_{,m} + \frac{J_w \Delta H_v}{T_{mf} - T_{mp}}} + \frac{1}{h_p}\right]^{-1} \text{ (51)}$$

The methodology adapted for the membrane distillation calculations needs to be further explained using mathematical models that are able to solve this kind of combination of linear and nonlinear equations. No doubt, the solution to simultaneous equations for heat flux gets time consuming and somewhat impossible to solve by hand as it involves a lot of variables and equations. Therefore, the methodology, needs to be also explained in terms of mathematical modelling. The mathematical model then, in turn is the main process which with the help of a software (MATLAB®), is able to perform complex calculations.

The next section of the thesis is the discussion and explanation of the mathematical model which describes the heat and mass transport in the membrane distillation system. After the discussion of the mathematical model, the real time experimental values obtained from the University of Aalborg regarding membrane distillation, will be portrayed and their results discussed.

4. Mathematical model for the description of heat transfer in Membrane Distillation

As a result of the preceding discussion, a comprehensive knowledge of the heat and mass transport mechanisms in DCMD is critical for improving our knowledge and future study in this sector. To increase our study and knowledge of the DCMD process, a number of unknowns must be discovered. These unknowns include heat transfer coefficients (h_f and h_p) of the boundary layers, the temperatures corresponding to membrane/liquid boundary (T_{mf} and T_{mp}), the conductive heat transfer coefficient of the membrane (h_m), the permeability of the membrane (B_m).

In most cases, the assessment of these unknowns is based on an empirical evaluation of the boundary layer heat transfer coefficients, followed by a basic thermal balance evaluation of the membrane/interface temperatures. The membrane heat transfer coefficient is calculated by the help of the thermal conductivities of the membrane polymer and the entrapped gas, which is established on membrane parameters such as permeability and depth. All these values are already combined in equation 43 to describe the formulation of the membrane heat transfer coefficient. But the parameters are dependent on the degree of crystallinity and temperature [55]. As a result, published figures in the literature might cover a wide range.

So, this requires a new approach to be tested which provides accurate, in a shorter range to be more pinpoint and more sure results. Hence, the approach adapted is based on the experimental values obtained from the DCMD experiments in which the system is evaluated at different temperatures, and two of them are used at a time. The subsequent equations obtained from this approach were then solved simultaneously for the unknowns using MATLAB® [52].

For the purpose of explanation of the mathematical model opted for the calculations, the subscripts in the coming equations refer to the DCMD experimental values for the bulk feed

temperatures i.e., T_{bf1} and T_{bf2}, correspondingly. It is also vital to note that the names and the subscripts of the variables that were used during the actual calculations could be different than the ones explained during the explanation of the mathematical model due the limitations of names of variables allowed in the software. Nevertheless, the MATLAB® code is attached in the appendix part of the thesis for a better understanding. Coming to the calculations and equation's part, the first step is to perform the energy balance at the corresponding temperature.

If we perform the energy balance at temperature that of T_{bf1}, it follows:

$$\dot{Q}_1 = M_{f1,in}\, H_{1,in} - M_{f,1out} H_{1,out} \quad (52)$$

In the equation 52, $\dot{Q}_1$ is the total heat transferred to the permeate side from the feed side in the system and is expressed in watts (W), $M_{f1,in}$, $M_{f,1out}$ represent the mass flow rates of the inlet and outlet of the at the feed and are expressed in (kg/s). the enthalpies are represented by $H_{1,in}$ and $H_{1,out}$ and correspond to the inlet and outlet enthalpies of the bulk feed and are expressed in (J/kg). The volumetric flow rate at the intake, as well as the temperature of the input and output streams, are all experimentally determined. After the temperatures are measured, the enthalpies of the streams are then looked up in the thermodynamic tables. All these values are used in the calculation of the outlet mass flow rate with the help of the mass balance equation:

$$M_{f1,out} = M_{f1,in} - J_w \rho A_m \quad (53)$$

Where in the equation, J_w represents the flux of water vapour (m/s), the membrane filtration area (m^2) is A_m and the flux density is represented by ρ (kg/m^3). As a result, The total heat transmitted in equation (52) divided by the membrane filtering area equals the heat flux. [52]. This value will then be utilised for the calculation of the unknowns in the following manner.

For the feed inlet temperature, $T_{bf1,in}$ the equations related to heat transfer can be written as the following:

$$Q_1 = h_{f1}(T_{bf1} - T_{mf1}) \quad (54)$$

$$Q_1 = h_{m1}\left(T_{mf1} - T_{mp1}\right) + J_{w1}\Delta H_v \quad (55)$$

$$Q_1 = h_{p1}(T_{mp1} - T_{bp1}) \quad (56)$$

Similar kind of equations can be written for the second feed inlet temperature and are as following:

$$Q_2 = h_{f2}(T_{bf2} - T_{mf2}) \text{ (57)}$$

$$Q_2 = h_{m2}\left(T_{mf2} - T_{mp2}\right) + J_{w2}\Delta H_v \text{ (58)}$$

$$Q_2 = h_{p2}(T_{mp2} - T_{bp2}) \text{ (59)}$$

Looking at the six equations (54-59), we find that the equations contain eight unknowns, which are the following:

1. h_{f1}
2. h_{f2}
3. h_{p1}
4. h_{p2}
5. T_{mf1}
6. T_{mf2}
7. T_{mp1}
8. T_{mp2}

ΔH_v can be obtained, which indicates the enthalpy of water per unit mass. The value of h_m can also be obtained from Eq (4). With the aim of solving the above system of equations with eight unknowns, we need to check for another two equations. With the use of empirical correlations of dimensionless numbers and the modification factors used to characterize the dependency of the viscosity of water, h_f and h_p, which correspond to the heat transfer coefficients can be determined [52].

The flow kind (laminar or turbulent) must be identified before selecting the appropriate empirical correlation. This may be accomplished by calculating the Reynolds number as shown below. The hydraulic diameter may be used to make a rough estimate of the Reynolds number [56]. Here it is important to mention that the Reynolds number can be mathematically defined as:

$$Re = \frac{vD_h\rho}{\mu} \text{ (60)}$$

Defining the variables in the equation, v is the velocity of the flow expressed in (m/s), the hydraulic diameter is expressed in (m) and is notated by D_h, and μ is the flow viscosity while ρ is the flow density expressed in (kg/m./s) and (kg/m^3) respectively. The Reynolds number helps in the determination of the flow whether the flow is laminar or turbulent. For Reynolds number less than 2300 , the flow is laminar, 2300 < Re < 4000 the flow is transient while the flow regime is determined to be turbulent is the Reynolds number is above 4000 for closed channel flows. In our experimental analysis, the Reynolds number tells us that the flow is laminar.

For the laminar flow regime, the empirical corelation is provided as:

$$Nu = 0.13Re^{0.64}Pr^{1/3} \quad (61)$$

Where Nu represents the Nusselt number, and Pr stands for the Prandtl number. To go into further detail about the two, Nusselt number is the ratio of convective to conductive heat transfer at a boundary of the fluid. While the Prandtl number is a dimensionless number like Nusselt and Reynolds which is ratio between the momentum diffusivity to thermal diffusivity.

For the inlet feed temperature, $T_{bf,1}$ the above-mentioned equation (61) can be revised for the heat transfer coefficient of the feed side of the system by the usage of the Nusselt number which is as follows:

$$h_{f1} = 0.13Re_1^{0.64}Pr_1^{\frac{1}{3}}(\frac{K_{f1}}{D_h}) \quad (62)$$

Where in the equation, the feed thermal conductivity is represented by k_{f1} at the temperature corresponding to the first temperature and D_h is the hydraulic diameter of the flow tube. In similar context, the inlet feed temperature, $T_{bf,2}$ can be stated as the following:

$$h_{f,2} = 0.13Re_2^{0.64}Pr_2^{1/3}(\frac{K_{f2}}{D_h}) \quad (63)$$

If we combine the equations (62 - 63), and rearranging the equations, we obtain the following corelation,

$$\frac{h_{f2}}{h_{f1}} = \frac{k_{bf2}}{k_{bf1}}\left(\frac{\rho_{bf2}\mu_{bf1}}{\rho_{bf1}\mu_{bf2}}\right)^{0.64}(\frac{Cp_{bf2}\mu_{bf,2}k_{bf,1}}{Cp_{bf1}\mu_{bf,1}k_{bf,2}})^{1/3} \quad (64)$$

The subscripts used in the equation (64) i.e., bf1, bf2, mf1 and mf2 are coincident to the temperatures T_{bf1}, T_{bf2}, T_{mf1} and T_{mf2} respectively. ρ is the density, while Cp and k are the heat capacity and the conductivity of the system. Last but not the least, μ represents the dynamic

viscosity of the water used in the system. The mentioned physical properties are evaluated at the provided temperatures.

Similarly, if we use the same approach for the for the permeate side, we can obtain a comparable formula for the heat transfer coefficients which can be stated as the following relation:

$$\frac{h_{p2}}{h_{p1}} = \frac{k_{bp2}}{k_{bp1}}\left(\frac{\rho_{bp2}\mu_{bp1}}{\rho_{bp1}\mu_{bp2}}\right)^{0.64}\left(\frac{Cp_{bp2}\mu_{bp,2}k_{bp,1}}{Cp_{bp1}\mu_{bp,1}k_{bp,2}}\right)^{1/3} \quad (65)$$

Now with a combination of the above 8 equations (54-59,64-65) we can solve all of the needed unknowns at the same time due to the fact that we have eight independent equations. Hence, the goal of this paradigm development, namely the assessment of the boundary layer heat transfer coefficients and membrane/liquid interface temperatures, has thus been accomplished.

It also worthwhile to note that one of the parameters involved in the evaluation, h_m, can be a factor to cause deviation in the obtained answer if it is not properly determined. As already stated, the determination of the parameter needs to be accurate and should be made sure that the solution does not diverge.

It is worth mentioning here that there are other mathematical models as well that exist for the calculation of the membrane distillation heat and mass transfer mechanisms. This method was adapted as the method involves the usage of experimental data and an easy-to-use derivations of formulas in the program. And the method is also tested to be proven to be more accurate as compared to other methodologies. The experimental data obtained from various experiments performed in the lab was used for the calculation of the unknown variables. To avoid any misconceptions of plagiarism and the sources of the data, it should be mentioned that the data obtained from the university of Aalborg in Denmark is being shared with the consent of the parties involved.

5. Experimental data and calculations

This section discusses the experimental values obtained for the membrane distillation experiments. The calculations then are performed over the obtained data and the mathematical model above comes into play for a major part of the evaluation. Majority of the values of the variables are already available in the literature of thermodynamics and obtained from thermodynamic tables corresponding to their respective temperatures. These values are majority of the same similar in different textbooks but may vary a few decimal places from literature to literature.

Nonetheless, as mentioned above several times, the calculation involves the usage of MATLAB® for performing solutions of simultaneous linear and nonlinear equations. The MATLAB® code used for the solution is attached in the appendix of the thesis for further consultation.

5.1 Experimental Data:

The experimental data along with the parameter of the system such as flow rates, area of membrane etc, are discussed as follows. For a little preview, the experiment was performed at three different temperatures of 40°C, 50°C and 60°C. The procedure was carried out for 120 minutes and the different values were recorded accordingly during the length of the experiment. The data recorded included various information but the data for interest for the thesis is the mass flow rate of the flow, flux of the water via the membrane, inlet and outlet temperatures of the feed and permeate side of the system. The starting volume of the feed and permeate side was also recorded along with the bath feed temperatures.

Other data recorded also includes the change of conductivity, water pH, the water recovery, the log mean temperature difference (LMTD), the standardized water flux and the XRD analysis of the water sample. Of the course the data obtained included the use of instrumentation to measure temperatures, flowrates, XRD, conductivity sensors, pH value sensors, stopwatch etc.

The following figure is a picture of the sample of water obtained from the demo site in Eilat, Israel.

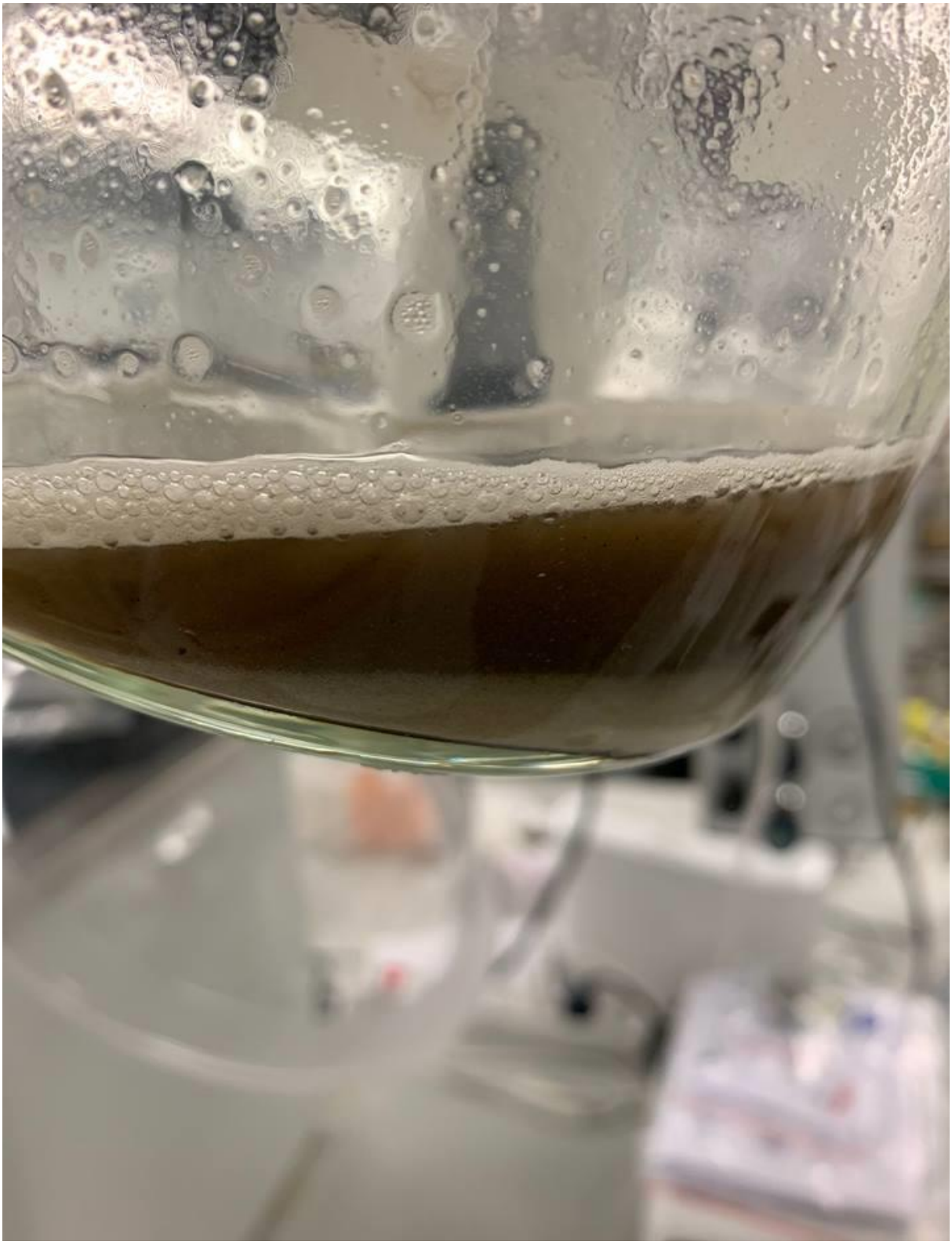

Figure 14: Picture of water sample obtained from the Demo site in Eilat, Israel.

The following tables depict the data of interest as mentioned above for the three temperatures. The data being shared in the thesis is confidential and is being shared after the consent of the conducting authority and obtaining permissions. The following table (7) is for values obtained at 60 degree Celsius.

		Feed Temperature		Permeate Temperature				
Time (min)	m (g)	Inlet (^{O}C)	Outlet (^{O}C)	Inlet (^{O}C)	Outlet (^{O}C)	Flow(ml)(every 10min)	Flow rate(ml/min)	LMH
0	237.12	54.1	34.1	26.1	34.9	0	0	0
10	272.77	55.8	38.5	24.5	38.7	35.65	3.565	2.139
20	310.81	56.8	39.3	24.6	40.1	38.04	3.804	2.2824
30	349.29	56.9	40	25.2	40.7	38.48	3.848	2.3088
40	381.65	56.7	40.8	25.5	40.5	32.36	3.236	1.9416
50	416.94	56.9	40.7	25.8	41.1	35.29	3.529	2.1174
60	450.29	56.9	41.8	26.1	39.8	33.35	3.335	2.001
70	480.14	57	42.1	25.9	38.4	29.85	2.985	1.791
80	510.64	57.1	41.8	25.7	38.2	30.5	3.05	1.83
90	539.74	57	42.5	25.5	37.3	29.1	2.91	1.746
100	568.84	57.1	43.3	25.2	36.7	29.1	2.91	1.746
110	598.63	56.6	43.3	25	37.1	29.79	2.979	1.7874
120	627.77	57.2	43.2	25.2	37.4	29.14	2.914	1.7484
Average value		56.62308	40.87692	25.40769	38.53077	30.05	3.005	1.803

Table 7: Experimental data obtained for 60 degrees temperature for membrane distillation

Similar values such as mentioned in the table above, were also obtained for 50 and 40 degrees respectively and are shown in the following tables (8-9).

		Feed Temperature		Permeate Temperature				
Time (min)	m (g)	Inlet (^{O}C)	Outlet (^{O}C)	Inlet (^{O}C)	Outlet (^{O}C)	Flow(ml)(every 10min)	Flow rate(ml/min)	LMH
0	231.02	47.2	35	24.6	31.5	0	0	0
10	268.88	47.3	34.8	23.7	32.6	37.86	3.786	2.2716
20	287.58	47.3	33.9	23.5	33.3	18.7	1.87	1.122
30	314.31	47.2	34	23.5	33.1	26.73	2.673	1.6038
40	339.08	47.2	34	23.5	32.6	24.77	2.477	1.4862
50	363.37	47.7	34.4	23.4	32.8	24.29	2.429	1.4574
60	386.66	47.4	34.7	23.3	31.7	23.29	2.329	1.3974
70	406.92	47.5	35.2	23.1	30.5	20.26	2.026	1.2156
80	427.1	47.7	35.6	22.9	29.6	20.18	2.018	1.2108
90	445.35	47.3	35.9	22.8	28.9	18.25	1.825	1.095
100	464.14	47.6	36.7	22.7	28.5	18.79	1.879	1.1274
110	481.62	47.5	37.4	22.7	28.5	17.48	1.748	1.0488
120	500.68	47.4	37.3	22.8	28.1	19.06	1.906	1.1436
Average value		47.40769	35.3	23.26923	30.9	22.47167	2.247167	1.3483

Table 8:Experimental data obtained for 50 degrees temperature for membrane distillation

		Feed Temperature		Permeate Temperature				
Time (min)	m (g)	Inlet (^{O}C)	Outlet (^{O}C)	Inlet (^{O}C)	Outlet (^{O}C)	Flow(ml)(every 10min)	Flow rate(ml/min)	LMH
0	230.22	38.2	28.5	22.4	27.3			
10	243.03	37.9	28.5	21.6	27.7	12.81	1.281	0.7686
20	256.96	38	28.4	22	27.7	13.93	1.393	0.8358
30	271.75	37.8	28.4	22.1	27.7	14.79	1.479	0.8874
40	285.53	37.7	28.5	22.2	27.7	13.78	1.378	0.8268
50	300.56	37.9	28.4	22.2	27.6	15.03	1.503	0.9018
60	316.46	38	28.6	22.3	27.4	15.9	1.59	0.954
70	331	38	28.5	22.3	27.6	14.54	1.454	0.8724
80	344.97	37.9	28.9	22.4	27.2	13.97	1.397	0.8382
90	356.95	38	29.6	22.3	26.3	11.98	1.198	0.7188
100	368.79	37.9	29.9	22.3	26.8	11.84	1.184	0.7104
110	380.62	38.2	30.2	22.3	25.8	11.83	1.183	0.7098
120	391.44	38.3	30.5	22.3	25.4	10.82	1.082	0.6492
Average value		37.98462	28.99231	22.20769	27.09231	13.435	1.3435	0.8061

Table 9:Experimental data obtained for 40 degrees temperature for membrane distillation

For the purpose of this thesis, the data extracted from the table 7, such that for 60 degrees is utilised.

5.2 Calculations for membrane distillation:

5.2.1 Evaluation of Temperatures, mass flow rate and enthalpies

Coming to the evaluation and starting of the calculations, we start from looking the values from the thermodynamic tables. Initially, as the temperatures are known, we find the average value of temperature for the two values that will be used in the calculations for both, the bulk feed and permeate side of the membrane. the following equations depict the procedure:

$$Avg\ Bulk\ feed\ temp_1 = T_{bf1} = \frac{T_{bf1in}+T_{bf1in}}{2} = \frac{55.8+38.5}{2} = 47.15^{O}C \text{ (66)}$$

$$Avg\ Bulk\ feed\ temp_2 = T_{bf2} = \frac{T_{bf2in}+T_{bf2in}}{2} = \frac{56.8+39.3}{2} = 48.05^{O}C \text{ (67)}$$

$$Avg\ Permeate\ feed\ Temp_1 = T_{bp1} = \frac{T_{bp1in}+T_{bp1in}}{2} = \frac{24.5+38.7}{2} = 31.6^{O}C \text{ (68)}$$

$$Avg\ Permeate\ feed\ Temp_1 = T_{bp2} = \frac{T_{bp2in}+T_{bp2in}}{2} = \frac{24.6+40.1}{2} = 32.35^{O}C \text{ (69)}$$

The above equations then help us in further calculations. Eq (66,67) are used for the calculations of enthalpy at the obtained temperature to be then used in equation (52) to obtain the total heat transferred to the permeate side from the feed side. The enthalpies H_{1in} and H_{1out} are obtained from the thermodynamic tables [57]. The following equations show the enthalpies obtained:

$$H_{1,in} = 233.6072\ KJ/Kg \text{ (70)}$$

$$H_{1,out} = 161.263\ KJ/Kg \text{ (71)}$$

The values are obtained by performing linear interpolations by using the values available in the table to obtain the above-mentioned values. Rewriting equation (52) to remember other values that need to be calculated:

$$\dot{Q}_1 = M_{f1,in}H_{1,in} - M_{f1,out}H_{1,out} \text{ (52,72)}$$

The equation requires the use of mass flow rates of the bulk feed as well. The mass flow rates are provided in the experimental data. The inlet mass flow rate at the bulk feed is equal to 19L/h. While the exit mass flow rate can be obtained by subtracting the flow that goes across the membrane from the original mass flow rate value. After performing the calculations, we obtain the following results:

$$M_{f1,in} = 19\,L/h = 5.32 \times 10^{-3} kg/s \text{ (73)}$$

The mass flow rate exiting the feed side is calculated the following way:

$$M_{f1,out} = M_{f1,in} - J_w \rho A_m = 5.32 \times 10^{-3} - 6 \times 10^{-5} = 5.26 \times 10^{-3}\ kg/s \text{ (74)}$$

Where in the above equation, J_w is the flux from the membrane, ρ is the flux density and A_m is the membrane filtration area. The filtration area is provided and is equal to:

$$Membrane\ Filtration\ Area = A = 0.1\ m^2 \text{ (75)}$$

Now the calculation for the heat transferred can be calculated. The value comes out to be:

$$\dot{Q}_1 = (5.32 \times 10^{-3})(233.6072) - (5.26 \times 10^{-3})(161.263) = 394.644\ J/s \text{ (76)}$$

To calculate the heat flux that is to be used in further calculations, we divide the heat transfer value by the membrane filtration area.

$$Q_1 = \frac{\dot{Q}_1}{A_m} = 3946.44\ W/m^2 \text{ (77)}$$

5.2.2 Calculation for Hydrophobic membrane heat transfer co-efficient

After the heat flux has been calculated, the hydrophobic membrane's heat transfer coefficient is calculated. The calculation requires the use of (k_m) and (k_g), which is the thermal conductivity of the hydrophobic membrane polymer, and air trapped inside the membrane pores respectively. As mentioned before in equation (43), the membrane heat transfer coefficient is calculated as follows:

$$h_{m1} = \frac{k_{g1}\varepsilon + k_{m1}(1-\varepsilon)}{\delta} = 213.00\, W/m^2\,.K \quad (78)$$

The porosity value ε is considered to be 0.51, the thickness of the membrane is taken as 450 x 10^{-6}m. These values were selected after carrying out a detailed review of the literature, as the values were not provided for calculations. The thermal conductivities were also chosen after consulting the literature for the type of membrane being used and then the hydrophobic membrane heat transfer coefficient was calculated. The assumed values for the thermal conductivities of air as well as the hydrophobic membrane can be found in appendix 1, in the MATLAB® code provided for the calculations. The values are dependent on temperature and hence vary from change in temperature.

The following figure depicts the influence of mean bulk temperature, T_{bf}, on h_m which is the conductive heat transfer coefficient of the membrane.

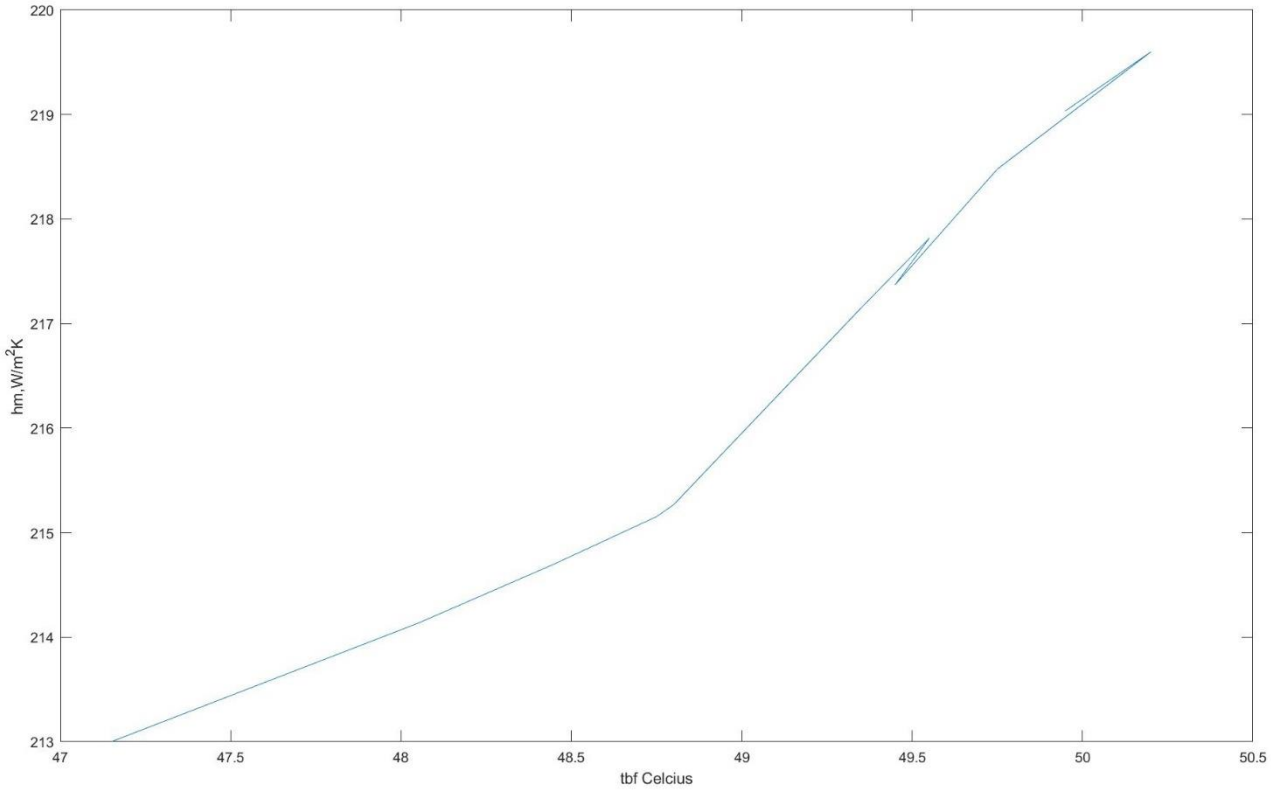

Figure 15: relation between tbf and hm

Figure 15 also demonstrates that as the average bulk temperature rises, the membrane heat transfer coefficient rises. The impact of water vapour in the pore on the membrane heat transfer coefficient is confirmed by the fact that the partial vapour pressure of water develops exponentially as the average temperature rises. Water vapour and polymeric materials' thermal conductivities both increase with temperature.

5.2.3 Evaluation of the FSOLVE command

The next steps of the calculations involve the use of the software MATLAB® for the solution of the unknowns in the eight simultaneous equations. The unknowns are the boundary layers' heat transfer coefficients (h_f and h_p), and the membrane /liquid interface temperatures (T_{mf} and T_{mp}) at each of the two chosen temperatures.

The generated MATLAB® application is primarily a system of eight equations (non-linear) that may be solved with MATLAB®'s built-in FSOLVE coding. The least square approach is used in this code to solve a system of nonlinear equations numerically. The FSOLVE coding was used to solve a pair of temperatures in the nonlinear equations system.

The code uses some initial guesses as well for the eight unknows, as it is a necessary requirement for the FSOLVE technique to obtain a solution. To further explain the procedure, the eight equations (54-59,64-65) mentioned above in the mathematical modelling of heat transfer of membrane distillation section and are transformed and used in a form that the syntax is valid for the FSOLVE command. The following figure shows the usage of the equations in a MATLAB® function used for calculation of FSOLVE command.

```
function Fun = MD(X)

Fun(1) =  X(1)*(47.15-X(2))-3946.44488115000098782392257135l4 ;
Fun(2) = (213*(X(2)-X(3)) + (5.941666666666662e-04*2388840))-3946.44488115000098782392257135l4;
Fun(3) = (X(4)*(X(3) - 31.6))-3946.44488115000098782392257135l4;
Fun(4) = (X(5)*(48.05-X(6)))- 3999.93158007200046365495245304O9;
Fun(5) = (2.141333333333334e+02*(X(6)-X(7)) + (0.000634000000000000*2386680))-3999.93158007200046365495245304O9;
Fun(6) = X(8)*(X(7) - 32.35)-3999.93158007200046365495245304O9;
Fun(7) = ((1.0059)- (X(5)/X(1)));%*((exp(-6.4313+(1882/X(2)))/(exp(-6.4313+(1882/X(6)))))^0.14));
Fun(8)= ((1.0048)-(X(8)/X(4)));%*((exp(-6.4313+(1882/X(3)))/(exp(-6.4313+(1882/X(7)))))^0.14));
end
```

Figure 16: Function Developed for the FSOLVE command portion of the calculation

5.2.4 Evaluation of the Evaporation Efficiency

Coming to the evaporation efficiency of the system, the parameter is a measure of the evaporation of the water in contact with the membrane on the permeate side and travelling to the permeate side. The efficiency tells us whether the membrane is working correctly in the conditions, or some changes are needed. Plus, the efficiency is a way to measure the performance of the system. Mathematically the efficiency can be expressed as done in equation (45). The evaporation efficiency in the DCMD process is defined as the ratio of heat transferred due to mass transfer to total heat transferred [52]. Because the permeate water vapour flow grew exponentially as the temperature increased, the evaporation efficiency and mass transfer contribution to the overall heat communicated increased as well. Talking about the evaporation efficiency obtained from the calculations after experimentation, the value ranged from around the 0.33 to 0.399. The values obtained for the evaporation efficiency follow the existing trend with some outliers. This may be due to several factors. Usually, the evaporation efficiency increases as the bulk feed temperature increases, but the calculations show some fluctuations caused by assumptions in the data set. It can also be due to errors is measuring the involved parameters. The following figures shows the relationship obtained between the EE and the tbf.

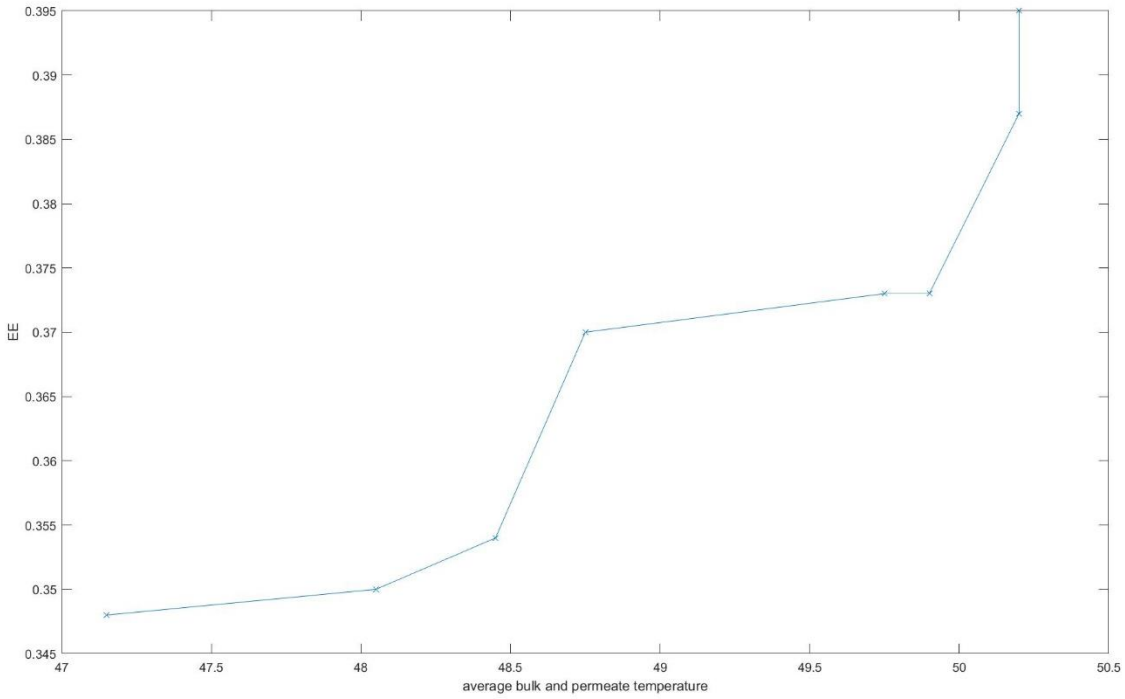

Figure 17: Relation Between tbf and EE

5.2.5 Evaluation of the temperature polarization co-efficient

The impact of raising the average bulk temperature (Tm) on the temperature polarization coefficient (TPC) is seen in figure.18. The results show that the TPC is reduces as the temperature increases. The trend obtained is following the trend that has been reported in the literature. The literature reports a decreasing trend of TPC when the average temperature is increased [58,59].

This pattern might be explained by the fact that as T_m rises, so does the amount of energy used by water vaporization at higher temperatures. As a result, the temperature polarization effect will be stronger, and the temperature polarization coefficient (TPC) will decrease. For well-designed systems, the TPC values can approach unity [60]. The high TPC values are owing to the high heat transfer coefficients of the boundary layers, which reflect the high feed and permeate flow rates as well as flow turbulence.

Figure 18: Relation between average bulk and permeate temperature and the TPC

6. Similar Comparative Technologies and their efficiencies

These section discusses the use of similar technologies that employ the filtration mechanisms

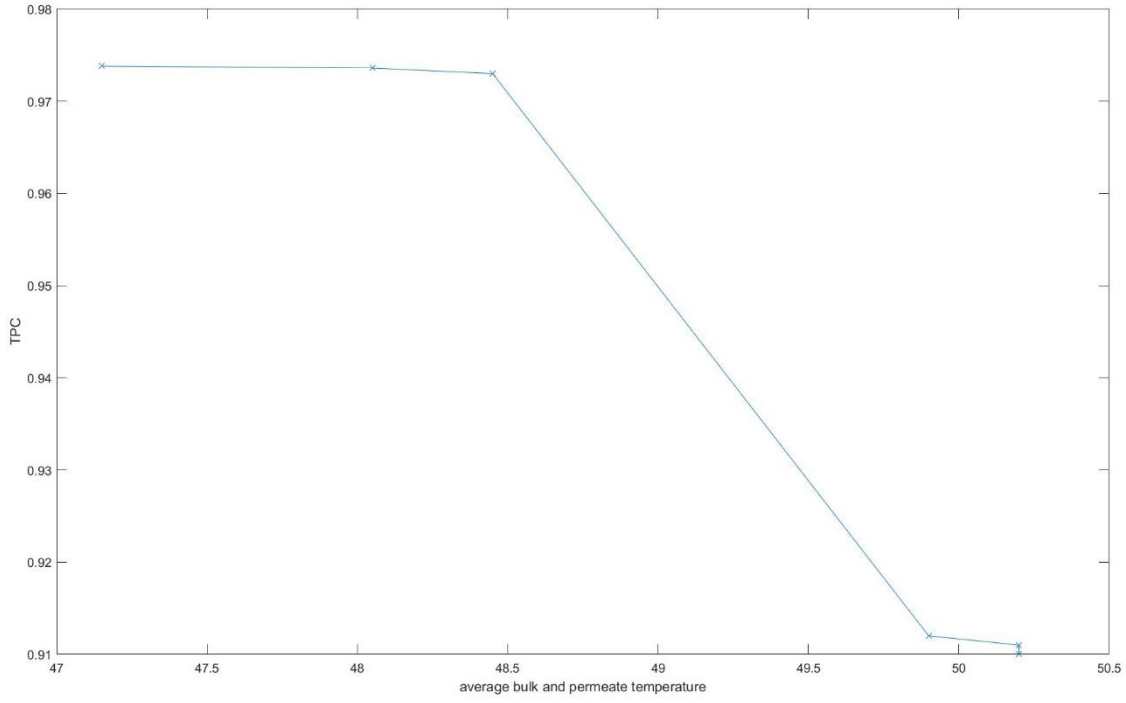

and are comparable to the membrane distillation procedure. The technologies to be discussed are the nano-filtration technology, and reverse osmosis. While the membrane distillation

technology is thermally driven, the other two technologies can be characterised as pressure driven procedures to perform more or less the same task.

This section caters for the efficiencies of these comparative technologies and how they can be calculated. Specially, talking about the thermal and mass transfer efficiency that can then be compared with the membrane distillation system values obtained from the demo site experimental analysis. This analysis helps in figuring out if the technology opted for the demo site is the more viable option or is there any other alternative that can perform better, and hence the technology could be replaced for further improved efficiency approximation.

6.2 Nano-Filtration

To dive into more detail, nano-filtration is a pressure-driven membrane separation technology that is commonly used for water softening is nanofiltration (NF) (i.e., separation of divalent and monovalent cations). The pore size of NF membranes, which ranges from 1 to 10 nm, is somewhat bigger than that of reverse osmosis membranes. The influence of the membrane charge should be included in the transport theory since the membrane is frequently charged.

The test the mass heat transfer efficiency, we check out the data obtained again from the university of Aalborg, Denmark for nano-filtration, for the demo site, in Eilat, Israel. For the calculation of the efficiencies, it is wise to use the same data for both the processes.

However, as mentioned above, the processes are similar but work of different thermodynamic principles, such that membrane distillation's working principle is thermally driven mass and heat transfer, and the nano-filtration technology works on pressure driven mass transfer to the permeate side. This being said, a MATLAB® program has been created for the calculation of the specific energy consumption of the nano-filtration technology which is placed in Puglia, Italy. Further explanation of the process at the demo site follows.

The desalinator portion of the device to be installed comprises of a nano-filtration module, which uses an industrially manufactured nano-filter. To put into context, in the tests conducted already in IRIS labs, the nano filter used was NF-90. The desalinator comprises of a nano-filtration unit, through which water is pumped through pipes according to the need of the hour. The efficiencies of the pumps are generally provided by the manufacturer in their range of operation. The output is the permeate and retentate. The latter refers to the water that is released

back in the ground or recirculated in the device for cleaning purposes and the permeate refers to the clean water obtained after filtration requirements are fulfilled.

To calculate that if the device is even feasible as an alternative method to the already installed systems to clean water, we calculate the SEC (specific energy consumption) of the Nano filtration procedure. The specific energy consumption (KWh/m^3) method is one of the basic approaches to calculate unit energy consumption of a product. In other words, it talks about the energy consumption requirements of the method to be used. The SEC can be considered one of the important parameters to check out the efficiency of the desalinator. Talking about the components of the desalinator device, e.g., filtration membrane, already is manufactured with pre-defined efficiencies under different working conditions.

Talking about the SEC in more detail, the parameter evaluates on the rather aspects of the usage of the machinery. After looking at the obtained values, one can then figure out if there is some other alternative system that might give better results under the same working conditions. SEC can then be paired with economical aspects of the project to calculate the overall cost of the project and its counterparts' alternative options.

Mathematically, the SEC can be defined by the following equation:

$$SEC = 2.778 \cdot 10^{-7} \frac{\Delta P \cdot Q_f}{Q_p} \quad (79)$$

Where in the above equation, ΔP (here expressed in $N\ m^{-2}$) represents the drop in pressure of the feed when it passes through the membrane module, 2.778×10^{-7} is the conversion factor from joules to kilowatt-hour, while volumetric flow rates of feed and permeate streams are represented by Q_f and Q_p respectively.

Coming to the financial aspects of the technology, when we consider the cost of the industrial energy in Eilat which is 0.15 €/kWh [5], we try to find a value of the SEC that will be produced to fulfil the energy needs of the system at a lower cost. For this purpose, a program written in MATLAB (Appendix 3) calculates different combinations of values for the feed flow rate and permeate flow rate that is desired . The specific cost for commercial freshwater in a region is 0.74€/m^3. Considering all the parameters and variables in the equation, and after comparison with alternative membranes used in the experiment, the NF 90 membrane is an attractive option for the production of freshwater from underground water in the area. The following figure depicts the relation between SEC and the specific cost.

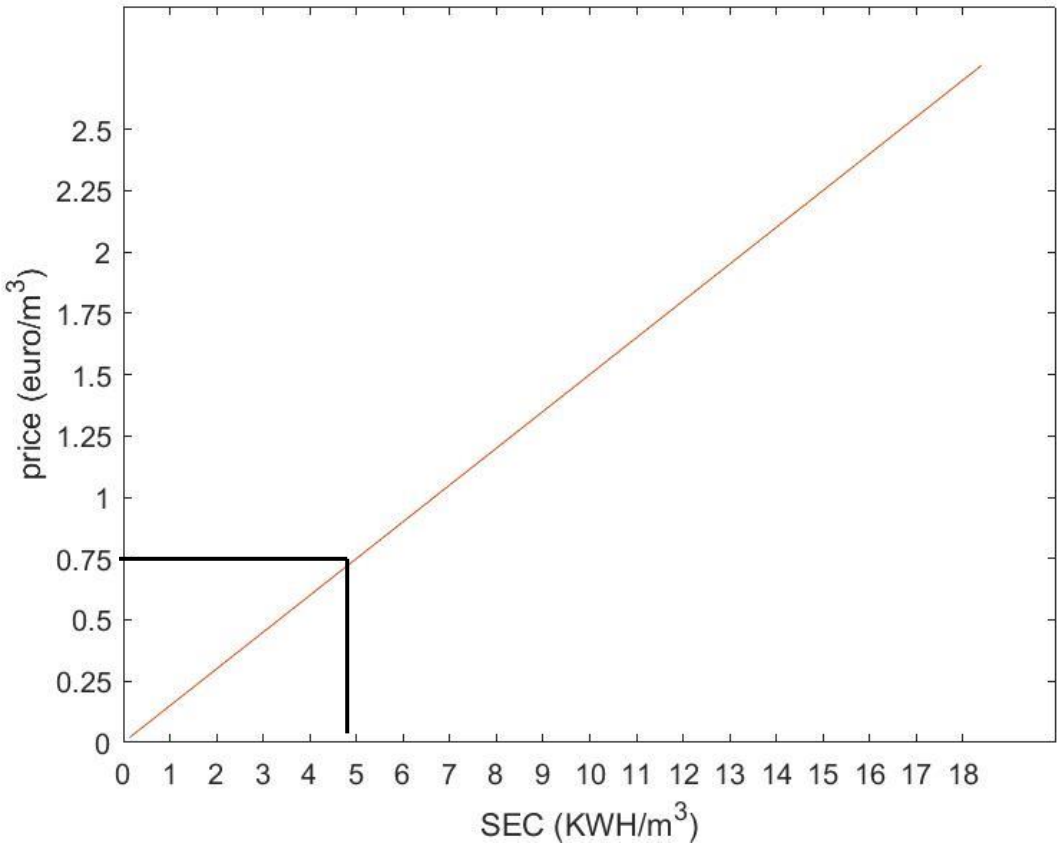

Figure 19: relation between SEC and price

So, after consulting the figure, any SEC below a cost of 0.74 euro/m^3 should be acceptable as it would be a cheaper alternative to the specific cost of commercial fresh water in Eilat [61]. Furthermore, the program also calculates various SEC values for a range of the flow rates and expected feed flow rate for a wider range of selection. Also, the system is not designed to work on a specific input of the feed flow rate, as the conditions might change according to demand or other hazards. The following diagram obtained from MATLAB calculates the SEC value for a range of input feed flow rates Q_f and defined working range of the membrane.

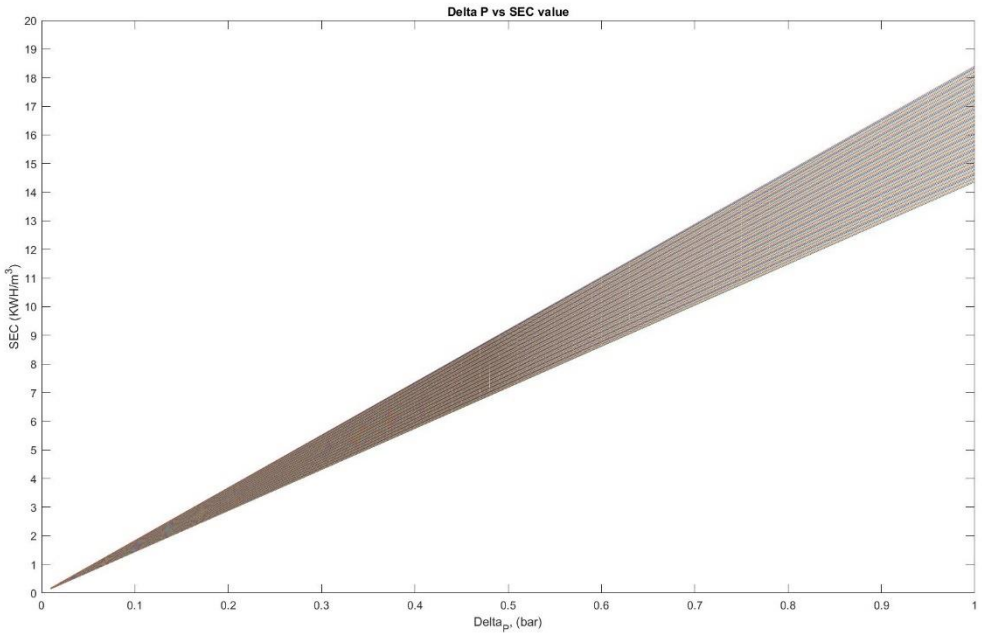

Figure 20: Relation between Pressure and SEC

The different lines in the figure about represent different SEC values obtained for various Q_f. consulting the figure for cost and flow rates, a range suitable for operation can be chosen in which the device would be profitable.

In an experiment conducted at the university of Aalborg which compared the membrane distillation technology with its counterpart nano-filtration, in a water defluorination process concluded that under the same testing conditions, the MD membrane allows for water fluxes that are one order of magnitude lower than those attained by NF; in other words, the area required by MD is around 10 times the area of its NF counterpart to filter the same quantity of water [62].

Still talking about the comparison of the two technologies, we need to check the water quality of the permeate water as well. Water systems in reality, on the other hand, can be described as complex mixtures of inorganic ions and organic molecules that frequently include living components. The permeability and selectivity of the two membranes toward fluoride ions should be compared in these types of systems. During the filtration process, they should be able to maintain their perm-selectivity. For example, in the same experiment the nano filtration membrane, which is a semi permeable membrane, was not very good at keeping the concentration of fluoride on the feed side. This is not surprising as the membrane is known to

be permeable to the fluoride F^- ions [63]. The optimal fluoride content in water is in the range of 0.5-1.0mg/L [64].

Membrane distillation, on the other hand, exhibits a larger drop in fluoride ion concentration despite the poor water production. It was reported in the experiment that the concentration was below the detection limit of the electrode (0.2ppm) even after the concentration was increased multiples times [62]. The experiment also discovered that the membrane distillation system had the capacity to retain completely the ions in question for feeds with a concentration as high as $1gL^{-1}$ [62].

To conclude the comparison, because the NF membrane is partly permeable to fluoride ions, it is not suited for treating streams with high fluoride concentrations, and the permeate may include fluoride levels that are unsafe for human consumption. Even when the membrane surface has been scaled and fouled, it has a substantially higher water production than the MD unit.

The most essential aspect of MD is that the feed quality is maintained throughout the filtration process, and the fluoride content in the permeate was under the electrode's detection limit (0.2 ppm). MD has a stronger fouling and scaling resistance than NF. It also doesn't require a lot of pressure, and it may be utilized to generate a vapour pressure differential across the membrane with solar or waste heat. MD's main drawbacks have been proved to be (i) poor water productivity and (ii) low permeate salinity, both of which must be adjusted to a safe level for human consumption. Current RO installations, on the other hand, are already experiencing similar issues.

The findings show that combining the two approaches in a synergistic manner might be a promising way to remediate fluoride-contaminated water. NF can be used to filter water until the fluoride ion concentration in the permeate fulfils local drinking water laws, or until fouling and scaling make the concentration process too unpleasant to continue, even with occasional backwashing. The quality of the generated drinking water degrades during concentration because NF membranes are partly permeable to fluoride ions. As a result, MD can be used to treat the NF concentrate. The MD process will benefit from NF preconcentration since it will reduce energy usage for heating and the membrane area. Cooling the MD concentrate crystallizes very pure CaF2, which may then be used in commercial operations like the generation of hydrogen fluoride. Furthermore, the permeates from the NF and MD modules

may be combined to provide high-quality drinking water with the specified fluoride ion and dissolved mineral concentrations.

6.3 Reverse Osmosis

Reverse osmosis (RO) is a water purification technology that uses a partially permeable membrane to remove ions, unwanted chemicals, and larger particles from drinking water. An applied pressure is utilized in reverse osmosis to counteract osmotic pressure, a colligative phenomenon generated by chemical potential differences in the solvent, a thermodynamic parameter.

Reverse osmosis is used in both industrial and drinkable water production to remove a wide spectrum of dissolved and suspended chemical species, as well as biological species (most notably bacteria) from water. Reverse osmosis is used in both industrial and drinkable water production to remove a wide spectrum of dissolved and suspended chemical species, as well as biological species (most notably bacteria) from water.

To briefly discuss the principles of reverse osmosis (RO), the RO membranes have no discernible holes that run the length of the membrane and are at the other end of the spectrum of commercially available membranes. Water must travel a difficult path across the membrane to reach the permeate side because the polymer substance of RO membranes produces a layered, web-like structure. RO membranes can reject the tiniest impurities, such as monovalent ions, whereas nanofiltration (NF), ultrafiltration (UF), and microfiltration (MF) membranes are intended to remove materials of increasing size [65].

Membranes can be employed in crossflow or dead-end filtering. RO membranes are primarily used in crossflow mode and come in spiral wrapped modules, which have the membrane sheets coiled around an inner tube that collects the permeate. The fluid is driven through the membrane by a positive hydrostatic pressure in most membranes, allowing filtering by pore flow. The fluid flow is determined by membrane porosity, which is the percentage of the membrane volume that is empty space and can hold liquid, and tortuosity, which is the distance a molecule must travel through the membrane divided by its thickness. Diffusion is also responsible for fluid transport via membranes.

However, diffusion controls transport via RO membranes, and there are no open channels for pore flow; the RO transport process is known as solution-diffusion transport. Unlike, Nano-

filtration membranes, in which the solvent transport takes place via a combination of convective and diffusive phenomenon.

In the solution-diffusion model, water transport across a RO membrane occurs in three phases: absorption onto the membrane surface, diffusion across the membrane thickness, and desorption from the permeate surface of the membrane. Once water molecules have absorbed onto the membrane surface, the water concentration gradient (of the water-membrane system) across the membrane causes them to diffuse down the concentration gradient to the permeate side of the membrane. The water molecule then desorbs from the membrane and mixes with the bulk permeate.

When it comes to the energy side of reverse osmosis, we need to know how much energy a desalination process uses. The first step is to familiarize yourself with the theoretical energy required to separate salt from water. This energy may be defined as the bare minimum required to separate salt and water using a technique. We employ the Gibbs free energy to our help from solution thermodynamics. It's worth noting that for mixing at constant temperature, the change in Gibbs free energy is always negative [66]. In other words, the total free energy of the components necessary to make the final mixture (salt, water, or salt-water combinations) is lower than the total free energy of the salt-water mixture. This is due to the fact that according to the second law of thermodynamics, the entropy of the system is increased due to spontaneous mixing.

Because salt-water mixing is a spontaneous process, the Gibbs free energy generated during mixing may be utilized to calculate the lowest amount of energy required to reverse the change. This is known as the thermodynamic minimum energy required for separation unmixing, and it may be determined using the following equation:

$$Min\ energy = d\left(\Delta G_{unmixing}\right) = -d\left(\Delta G_{mixing}\right) = \pi_s \bar{V}_w dn_w \quad (80)$$

Where $\Delta G_{unmixing}$ is the Gibbs free energy of unmixing expressed in Joules or KWh/m^3, ΔG_{mixing} is the Gibbs free energy of mixing expressed in the same units, π_s refers to the osmotic pressure of the salt-water mixture expressed in pascals, $\bar{V}_w$ is the molar volume of water expressed in m^3/mol and n_w is the moles of water participating in the mixture. In context of the separation process, the unmixing is specified as recovery and the equation (80) caters for infinitesimally small portions such that recovery of a small portion of water from the solution.

The equation can then be integrated over a specified water recovery R to get the least amount energy necessary by the following equation:

$$E_{Thermodynamic\ minimum} = \frac{1}{R}\int_0^R \pi dR \quad (81)$$

Where in the equation, R refers to the recovery of the amount of water. Indeed, if you know the initial feed concentration, ion composition, and temperature, you can calculate osmotic pressure as a function of different recoveries to generate osmotic curves like the one shown in figure.

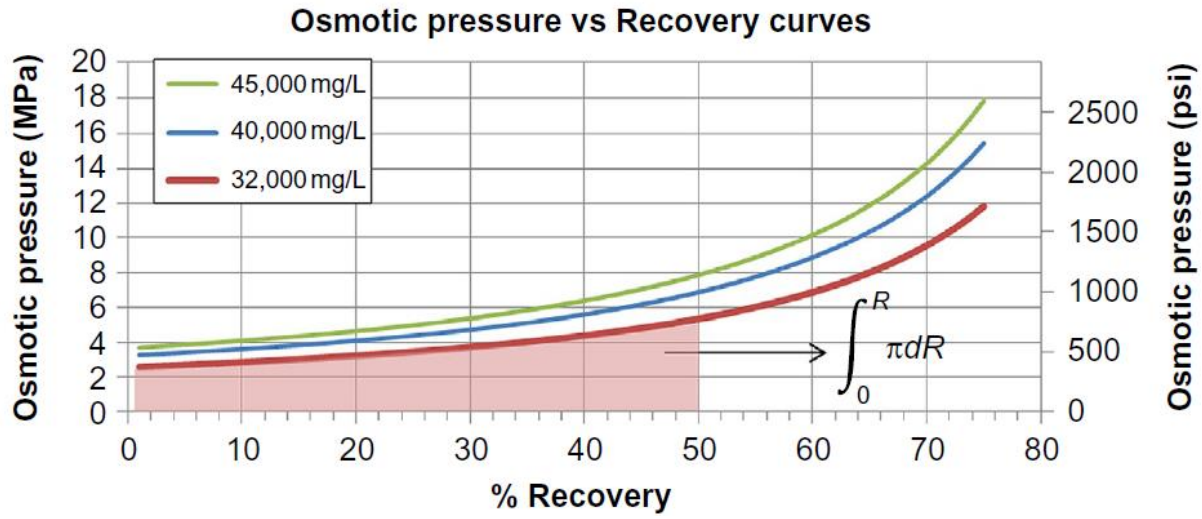

Figure 21:osmotic pressure vs recovery for different feed concentrations typical of sea water feed [66].

It is to be understood that the $E_{thermodynamicminimum}$ that is required for the separation is not achievable due to the losses incurred. To define the efficiency of the reverse osmosis pressure or desalination procedures in general, it can be given by:

$$\eta_E = \frac{E_{thermodynamicminimum}}{E_{thermodynamicminimum+W}} \quad (82)$$

Where W is the work done expressed in joules of KWh/m^3. Considering the equation (82), and other types of energies that are required for the process to work, for example, to generate the flux, there is a need to provide energy, also for rejection through a membrane, energy is also consumed inside the modules that accounts for the polarization of the concentration, the very important pressure drop for the whole system to work has to be also supplied by the power source. When talking about reverse osmosis, this power source is a pressure pump.

When we talk about sea water desalination, the typical recoveries indicated in the literature are around 50 percent while it is possible that the feed pressures will be in excess of 800 psi

(55bars). While this is not true for the membrane distillation, during the experiment, the water recovery factor reached around a maximum of 80 percent after 1020 minutes.

Because of the extremely high pressures obtained in the reverse osmosis process, a large quantity of energy must be recovered before disposal. Usually, the systems are fitted with energy recovery devices. The preferred devices being pressure or work exchangers. It is important that the system is synchronized after consideration of appropriate operating ranges so that the pumps and energy recovery devices can work at a maximum efficiency without hindering normal operations. If we look at the reported efficiencies, the reported values range from >95% without any bad or adverse effects on the feed.

Finally, if we talk about the electrical energy needed for the pumps that are used in reverse osmosis, the electrical energy is the output of a power plant. Typically, power plants use fuel or chemical energy as a source of energy. In the United States, coal and natural gas account for more than 60% of the energy sources for power plants, with coal accounting for more than 40%, followed by natural gas, nuclear power, oil, hydro, and renewables [65,66].

These power cycles have an efficiency that varies from 27 percent to 42 percent for coal-fired power plants, 33 percent to 55 percent for natural-gas-fired power plants, and 24 percent to 44 percent for oil-fired power plants. As a result, when comparing the energy efficiency of reverse osmosis to that of thermal desalination, this efficiency must be considered because thermal plants employ both heat and electricity as a source of energy.

According to the analysis, the energy efficiency of reverse osmosis, as determined by Eq. (83), which is effectively Eq. (82) renamed for reverse osmosis, is about 53%, with the remaining 47% accounted for by thermodynamic minimum energy. The remaining energy is accounted for by the work term WRO, which can be defined as the total amount of work done to create membrane flux, overcome module configuration, friction, and concentration polarization losses, as well as overcome pump losses, energy recovery device losses, and system friction losses [66].

$$\eta_{E,RO} = \frac{\mathrm{E}_{\mathrm{thermodynamicminimum}}}{E_{\mathrm{thermodynamicminimum}} + W_{RO}} \quad (83)$$

To conclude the reverse osmosis efficiency phenomenon, the unit has around 50% of energy efficiency with electrical energy as input. Thermodynamics accounts for half of the energy use,

thereby cutting any additional advances in half right away. Pumps and energy recovery systems, which account for the remaining 28% of energy losses, are already exceedingly efficient. As a result, 75 percent of overall energy use cannot be further reduced. Membranes and modules make up the remaining 25%, with membranes accounting for 15% and modules for 10%. Membrane innovation will yield some energy savings, but not at a system scale, and various evaluations imply that high permeability membranes for both seawater and brackish water reverse osmosis desalination have already reached a point of diminishing returns for energy reductions [66].

7.Specific Energy Consumption (SEC) Comparison of the Technologies

Specific energy consumption can be defined as the ratio of energy in KWh (Kilowatt-hours) that is consumed to the output weight or quantity of the product that is produced due this consumption of energy [69]. The parameter expressed in KWh/m^3 is regarded as a key parameter in assessing the overall feasibility of the process of desalination. This section compares the overall values of the specific energy consumption of the three technologies discussed above.

As the above discussed technologies differ in the driving mechanism of the technology, such that the membrane distillation is a thermally driven process while the other two work on the principle of pressure difference, it is not a very good idea to measure the thermodynamic efficiencies of the systems for a comparison. Therefore, the SEC value is a better comparison strategy among the three technologies.

This section discusses the specific energy consumption of the three technologies. Whether the technology is feasible for the requirements of the demo site, whether it is financially sustainable to deploy membrane distillation or reverse osmosis or even nano filtration as the desalination process of choice. But one important prospect should be kept in mind that specific energy consumption can only provide us with the energy consumption analysis, not the qualitative analysis of water treatment which entails the composition of the desalinated water. As the thesis mainly focuses on the energy consumed by the three process and their efficiency, specific energy consumption is a good parameter to be compared among the technologies. The following section discusses the SEC values for the three technologies.

7.1 Membrane distillation SEC

Membrane distillation, like various other thermal processes, relies on a substantial value for thermal energy for generating vapour of water from its liquid phase. As an alternative the waste heat from the industrial processes or solar energy could be potentially an alternate energy source for powering the system. The MD process has received a lot of attention in the last decade because of its low energy requirements and high-quality water production. It's been considered as a possible alternative to thermal desalination and the SWRO (Seawater Reverse Osmosis) process, or in combination with traditional desalination techniques to lower operating costs and energy requirements.

In consideration of the sustainability of the process, membrane distillation has a huge drawback and technical problems, in terms of thigh energy demand that creates a substantial number of pollutants and harmful pollutants. These flaws necessitate the search for more environmentally benign, long-term desalination methods.

Here it is rather important note that there is a difference between the thermal energy and electrical energy. While both the quantities are measured in kilowatt-hours (KWh), the two quantities are not directly comparable. In a typical thermal power plant, energy is transformed from chemical to thermal to mechanical to electrical energy to create electrical energy (kWh_e). The straight comparison of thermal energy (kWh_{th}) and electrical energy (kWh_e) is improper since each energy transition incurs some efficiency loss. We used the Semiat relationship to convert reported thermal energy values to comparable electrical energy values for this investigation, assuming a contemporary power plant efficiency of 45 percent, such that the relation obtained can be mathematically expressed as:

$$kWh/m^3 = KWh_e/m^3 + 0.45kWh_{th}/m^3 \quad (84)$$

Now the following table displays the SEC values for the various thermal and membrane desalination processes:

Technology	Specific Energy Consumption (kWh/m^3)		
	Electric	Thermal	Total Electric Equivalent
BWRO	0.5–3	–	0.5–3
SWRO	3–6	–	3–6
ED	1–3.5	–	1–3.5
EDR	1–2	–	1–2
MVC	7–15	–	7–15
FO	0.2–0.5	20–150	10–68
MD	1.5–4	4–40	3–22
MSF	2.5–5	40–120	21–59
MED	2–2.5	30–120	15–57
MEB	2	60	30

Figure 22: SEC Values for different desalination procedures[70]

Hogan et al. from the University of New South Wales were the first to publish their findings, which used a 3 m2 flat plate solar collector and a hollow fibre membrane MD system with a capacity of 0.05 m^3/day. The system used 55.6 kWh/m^3 of total energy and produced a water vapour flow of 17/day.m^2 of collector area, which is quite similar to what has been reported for solar multi-stage flash distillation and multiple-effect distillation.

7.2 Reverse Osmosis SEC

The specific energy consumption of the RO process is closely linked with the treatment capacity of the plant. In large facilities, efficiency gains linked to pumps can be beneficial, and depending on the capacity, energy recovery devices provide useful reduction in the SEC. Pelton turbines, for example, can save 35–42 percent energy in plants with capacities less than 5000 m^3/day, but isobaric energy recovery devices may decrease SEC by 55–60 percent in plants with capacities more than 5000 m^3/day. In facilities with capacities less than 5000 m^3/day, Pelton turbines can save 35–42 percent energy, while isobaric energy recovery devices may reduce SEC by 55–60 percent in plants with capacities more than 5000 m^3/day. According to thermodynamic calculations, the minimal specific energy consumption for a 35Kppm feed system with 50% recovery is around 1.06 kWh/m^3. The specific energy consumption of seawater reverse osmosis system can also be seen in figure 22.

The pressure differential across the membrane must theoretically surpass 2.51 MPa (24.8 atm), and the minimum effort required to create 1000 cm^3 water is 0.7Wh/L (0.7 kWh/m3). As the system recovery (ratio of product to feed water flow) approaches zero, this reflects the lower limit of the work investment. Similarly, the theoretical minimal SEC was calculated to be around 0.2 kWh/m^3.

The technology for reduction of SEC for reverse osmosis systems has come a long way. The energy footprint of RO processes has fallen from 20 kWh/m^3 in the 1970s to less than 2 kWh/m^3 now for saltwater desalination and roughly 1 kWh/m^3 for brackish water desalination. Exergy study of several RO systems aided in the development of a more efficient energy system. The SEC of commercial SWRO systems has dropped over time, decreasing from an average of 20 kWh/m^3 in 1980 to 1.62 kWh/m^3 in 2005, as it did for many other desalination methods. Although the ideal SEC for desalination increases as temperature rises, the opposite is true in actual RO systems as salt and water fluxes rise with higher temperatures, with diffusion through the membranes increasing at an estimated rate of 3% to 5% per degree Celsius up to varying limits of commercial membranes, resulting in a reduction in SEC.

8. Conclusion and Discussion

In line with the research proposed in the first chapter of the thesis, we provided a brief overview of some of the current technologies available in the market for filtration with emphasis on membrane distillation. A detailed literature review was discussed for membrane distillation as the main focus of the thesis was to discuss the theory for the efficiency of membrane distillation in terms of heat and mass transfer, and experimental results obtained for the water samples taken from the demo site in Eilat, Israel. The experimental values were then taken from the lab of the university of Aalborg which is a partner in the European project named project Ô. The values obtained proved to be extremely helpful in figuring out the efficiency parameters for the membrane distillation system installed at the demo site. We need to keep in mind that the analysis was carried out using experimental data only and the real time values could not be obtained from the working site as the demo site is still under construction phase. This delay is due to the ongoing COVID-19 pandemic that has affected the whole world and has proved fatal for businesses and manufacturing companies globally.

The benefits of using performance metrics for performance measurement of machinery are visible. Not only do they provide a metric for us to weigh the pros and cons of the system in use, but they also help us to create a maintenance framework for the machinery in question. Performance metrics like efficiencies etc. can be a grounds for comparison of similar kinds of machines, whether a machine can be replaced with its counterpart, the replacement will even prove beneficial for all the stake holders involved, or maybe some modification in the system will provide with a better and improved overall result.

The purpose of this thesis was to analyse the membrane distillation system to be installed at the demo site in Eilat, Israel with the main concern for the efficiency of the system. As the system main task is to filter out the salt contents of water coming in which has already been passed through various systems for removal of organic and non-organic matter, we focus mainly on the evaporation efficiency and temperature polarization of the system. These two factors play an important role in checking whether the system is a viable option to be installed at the demo site. Also, membrane distillation has an extremely large advantage of the rival counterpart systems of nano-filtration and reverse osmosis, and that is water recovery. As discussed previously, the water recovery from reverse osmosis and nano-filtration is alike. Modern reverse osmosis and nano-filtration systems can provide up to a recovery of 50% of the total

feed at the inlet while in our experiments for the membrane distillation system, the water recovery factor was almost 80% (Appendix 4.)

Talking about the efficiencies of the systems and comparing them, the evaporation efficiency of the system for membrane distillation came out to be in the range of 0.33 to 0.399. So probably if the system is meant to be working at lower temperatures, it will be viable if only a cheap source of heating power is available for the system to work. This factor is well covered as the demo site will be installed with solar panels to provide energy for the system to work as the area lies in the middle east and experiences a lot of sunshine at high temperatures. Other than, that the temperature polarization coefficient obtained from the experimental data was high and around the range of 0.91 to 0.98. The value for temperature polarization implies that the system did not experience a lot of temperature polarization for some temperatures while some values proved to create a polarization effect in the system.

Coming to the working mechanisms of the systems, membrane distillation system is basically a thermally driven system which relies on temperature. This introduces a partial pressure affect in the system between the two flows, feed and permeate across the membrane, causing the vapour molecules to be transferred from the membrane pores from an area of high partial pressure to an area of low partial pressure and as the vapour pressure difference between the two membrane sides is maintained, and they are finally condensed either internally downstream of the membrane or externally outside the membrane module. While the other two systems discussed, nano-filtration and reverse osmosis are pressure driven systems which rely on pressure difference to start the filtration process and do not use a hydrophobic membrane like in membrane distillation.

To conclude the discussion, membrane distillation can be a viable option only if several factors are met. These factors include the size of the system to be installed according to the need as previously mentioned, as compared to reverse osmosis, a significantly larger membrane system is required to be installed to perform the same job, the power requirements pertaining to electrical and thermal power are also to be taken into effect.

Incorporating plasmonic and nanophotonic materials on the membrane surface, followed by irradiation with UV light or sunshine, can boost the capacity of MD processes on a small scale. In vacuum MD, adding plasmonic nanoparticles to the membrane increases the water vapour flow by 11 times, and the temperature at the membrane interface is greater than the bulk temperature. These low-capacity portable MD desalination devices would be ideal for locations

with limited electric energy supply or availability. However, improving low driving forces remains a significant problem that must be addressed before MD desalination systems can be used effectively. Plus, membrane distillation is claimed to be more fouling resistance as compared to the counter-part reverse osmosis.

Lastly, in terms of cleaning the water, membrane distillation systems perform the best. The systems can stop majority of the salts such as fluoride salts in the water which can easily seep through while using pressure driven systems like nano-filtration. Hence pressure driven system require a continuous step wise approach to clean the water in turns whereas one membrane distillation system can provide with same or better results.

8.1 Delimitations:

There is no doubting that COVID-19 has been disastrous for all enterprises and industrial firms throughout the world. This has proved as a delimitation in my work as I was not able to visit the labs for experimentation, the demo site for collection of samples as well. Plus, the pandemic has also delayed the work on the project by quite some time which meant that only experimental data was available for performing calculations while the real-time values are still not obtainable as the demo site is still under construction. I did my best to make the most of the information I had and to offer valuable insights into the behaviour of the membrane distillation system under investigation.

BIBLIOGRAPHY

[1] M. Khayet and T. Matsuura, "Introduction to Membrane Distillation," *Membr. Distill.*, pp. 1–16, 2011, doi: 10.1016/b978-0-444-53126-1.10001-6.

[2] A. Alhathal Alanezi *et al.*, "Theoretical investigation of vapor transport mechanism using tubular membrane distillation module," *Membranes (Basel).*, vol. 11, no. 8, 2021, doi: 10.3390/membranes11080560.

[3] A. A. Alanezi, M. R. Safaei, M. Goodarzi, and Y. Elhenawy, "The effect of inclination angle and reynolds number on the performance of a direct contact membrane distillation (DCMD) process," *Energies*, vol. 13, no. 11, pp. 1–16, 2020, doi: 10.3390/en13112824.

[4] A. Alkhudhiri, N. Darwish, and N. Hilal, "Membrane distillation : A comprehensive review," vol. 287, pp. 2–18, 2012, doi: 10.1016/j.desal.2011.08.027.

[5] X. Ma, C. A. Quist-Jensen, A. Ali, and V. Boffa, "Desalination of groundwater from a well in puglia region (Italy) by al2o3-doped silica and polymeric nanofiltration membranes," *Nanomaterials*, vol. 10, no. 9, pp. 1–12, 2020, doi: 10.3390/nano10091738.

[6] E. Nagy, "Chapter 20 - Reverse Osmosis," *Basic Equations Mass Transp. Through a Membr. Layer*, no. 1962, pp. 497–503, 2019, doi: 10.1016/B978-0-12-813722-2.00020-0.

[7] J. A. G. Thomas, "Energy analysis," *Energy Anal.*, pp. 1–162, 2019, doi: 10.4324/9780429051937.

[8] M. Iwase, *First, Second, and Third Laws of Thermochemistry*, vol. 1. Elsevier Ltd., 2013.

[9] M. C. García-Payo, M. A. Izquierdo-Gil, and C. Fernández-Pineda, "Air gap membrane distillation of aqueous alcohol solutions," *J. Memb. Sci.*, vol. 169, no. 1, pp. 61–80, 2000, doi: 10.1016/S0376-7388(99)00326-9.

[10] M. Khayet, "Membranes and theoretical modeling of membrane distillation: A review," *Adv. Colloid Interface Sci.*, vol. 164, no. 1–2, pp. 56–88, 2011, doi: 10.1016/j.cis.2010.09.005.

[11] D. R. L. Kevin W. Lawson, “Membrane Distillation,” *Nanostructured Polym. Membr.*, vol. 1, pp. 419–455, 2016, doi: 10.1002/9781118831779.ch11.

[12] C. Gostoli and G. C. Sarti, “Separation of liquid mixtures by membrane distillation,” *J. Memb. Sci.*, vol. 41, no. C, pp. 211–224, 1989, doi: 10.1016/S0376-7388(00)82403-5.

[13] F. Laganà, G. Barbieri, and E. Drioli, “Direct contact membrane distillation: Modelling and concentration experiments,” *J. Memb. Sci.*, vol. 166, no. 1, pp. 1–11, 2000, doi: 10.1016/S0376-7388(99)00234-3.

[14] M. Khayet, C. Y. Feng, K. C. Khulbe, and T. Matsuura, “Preparation and characterization of polyvinylidene fluoride hollow fiber membranes for ultrafiltration,” *Polymer (Guildf).*, vol. 43, no. 14, pp. 3879–3890, 2002, doi: 10.1016/S0032-3861(02)00237-9.

[15] S. Srisurichan, R. Jiraratananon, and A. G. Fane, “Mass transfer mechanisms and transport resistances in direct contact membrane distillation process,” *J. Memb. Sci.*, vol. 277, no. 1–2, pp. 186–194, 2006, doi: 10.1016/j.memsci.2005.10.028.

[16] J. Phattaranawik, R. Jiraratananon, and A. G. Fane, “Heat transport and membrane distillation coefficients in direct contact membrane distillation,” *J. Memb. Sci.*, vol. 212, no. 1–2, pp. 177–193, 2003, doi: 10.1016/S0376-7388(02)00498-2.

[17] M. Khayet, T. Matsuura, J. I. Mengual, and M. Qtaishat, “Design of novel direct contact membrane distillation membranes,” *Desalination*, vol. 192, no. 1–3, pp. 105–111, 2006, doi: 10.1016/j.desal.2005.06.047.

[18] K. Schneider and T. J. van Gassel, “Membrandestillation,” *Chemie Ing. Tech.*, vol. 56, no. 7, pp. 514–521, 1984, doi: 10.1002/cite.330560703.

[19] M. Khayet, A. Velázquez, and J. I. Mengual, “Modelling mass transport through a porous partition: Effect of pore size distribution,” *J. Non-Equilibrium Thermodyn.*, vol. 29, no. 3, pp. 279–299, 2004, doi: 10.1515/JNETDY.2004.055.

[20] L. Marťinez, F. J. Florido-Ďiaz, A. Herńandez, and P. Prádanos, “Estimation of vapor transfer coefficient of hydrophobic porous membranes for applications in membrane distillation,” *Sep. Purif. Technol.*, vol. 33, no. 1, pp. 45–55, 2003, doi: 10.1016/S1383-5866(02)00218-6.

[21] F. A. Banat and J. Simandl, “Theoretical and experimental study in membrane

distillation," *Desalination*, vol. 95, no. 1, pp. 39–52, 1994, doi: 10.1016/0011-9164(94)00005-0.

[22] S. Hsu, K. Cheng, and J. Chiou, "Seawater desalination by direct contact membrane distillation," *Desalination*, vol. 143, pp. 279–287, Jun. 2002, doi: 10.1016/S0011-9164(02)00266-7.

[23] Z. Ding, R. Ma, and A. G. Fane, "A new model for mass transfer in direct contact membrane distillation," *Desalination*, vol. 151, no. 3, pp. 217–227, 2003, doi: 10.1016/S0011-9164(02)01014-7.

[24] C. M. Guijt, I. G. Rácz, J. W. Van Heuven, T. Reith, and A. B. De Haan, "Modelling of a transmembrane evaporation module for desalination of seawater," *Desalination*, vol. 126, no. 1–3, pp. 119–125, 1999, doi: 10.1016/S0011-9164(99)00163-0.

[25] R. W. Schofield, A. G. Fane, and R. Macoun, "Factors Affecting Flux in Membrane Distillation," vol. 77, pp. 279–294, 1990.

[26] M. I. Va, "Temperature and concentration polarization in membrane distillation of aqueous salt solutions," vol. 156, 1999.

[27] Y. Yun, R. Ma, W. Zhang, A. G. Fane, and J. Li, "Direct contact membrane distillation mechanism for high concentration NaCl solutions," vol. 188, no. February 2005, pp. 251–262, 2006, doi: 10.1016/j.desal.2005.04.123.

[28] P. Termpiyakul and R. Jiraratananon, "Heat and mass transfer characteristics of a direct contact membrane distillation process for desalination," vol. 177, pp. 133–141, 2005, doi: 10.1016/j.desal.2004.11.019.

[29] J. Phattaranawik and R. Jiraratananon, "Direct contact membrane distillation : effect of mass transfer on heat transfer," vol. 188, pp. 137–143, 2001.

[30] E. Drioli and F. Matera, "Dept. of Chemistry, C&m. Eng. Sect., University of Calabria I-87030 Arcavacata di RENDE (CS)," vol. 83, pp. 209–224, 1991.

[31] L. Martínez-Díez and M. I. Vázquez-González, "Effects of polarization on mass transport through hydrophobie porous membranes," *Ind. Eng. Chem. Res.*, vol. 37, no. 10, pp. 4128–4135, 1998, doi: 10.1021/ie970911q.

[32] G. C. Sarti, C. Gostoli, and S. Matuili, "LOW E N E R G Y COST DESALINATION

PROCESSES," vol. 56, pp. 277–286, 1985.

[33] A. M. Alklaibi and N. Lior, "Membrane-distillation desalination: status and potential," vol. 171, pp. 111–131, 2004, doi: 10.1016/j.desal.2004.03.024.

[34] S. Gunko, S. Verbych, M. Bryk, and N. Hilal, "Concentration of apple juice using direct contact membrane distillation," vol. 190, pp. 117–124, 2006, doi: 10.1016/j.desal.2005.09.001.

[35] T. Chen, C. Ho, and H. Yeh, "Theoretical modeling and experimental analysis of direct contact membrane distillation," vol. 330, pp. 279–287, 2009, doi: 10.1016/j.memsci.2008.12.063.

[36] M. Matheswaran, T. O. Kwon, J. W. Kim, and I. S. Moon, "Factors Affecting Flux and Water Separation Performance in Air Gap Membrane Distillation," no. May, 2014.

[37] L. Martlnez, "Comparison of membrane distillation performance using different feeds," vol. 168, pp. 359–365, 2004.

[38] M. Tomaszewska, M. Gryta, and A. W. Morawski, "Study on the concentration of acids by membrane distillation," vol. 102, pp. 113–122, 1995.

[39] A. M. Alklaibi and N. Lior, "Transport analysis of air-gap membrane distillation," vol. 255, no. April 2004, pp. 239–253, 2005, doi: 10.1016/j.memsci.2005.01.038.

[40] F. A. Banat and J. Simandl, "Separation Science and Technology Desalination by Membrane Distillation : A Parametric Study," no. October 2014, pp. 37–41, doi: 10.1080/01496399808544764.

[41] X. L. Zhang, W. D. Zhang, X. M. Hao, H. F. Zhang, Z. T. Zhang, and J. C. Zhang, "Mathematical model of gas permeation through PTFE porous membrane and the effect of membrane pore structure," *Chinese J. Chem. Eng.*, vol. 11, pp. 383–387, Aug. 2003.

[42] A. W. Mohammad, Y. H. Teow, W. L. Ang, Y. T. Chung, D. L. Oatley-Radcliffe, and N. Hilal, "Nanofiltration membranes review: Recent advances and future prospects," *Desalination*, vol. 356, pp. 226–254, 2015, doi: 10.1016/j.desal.2014.10.043.

[43] W. M. Deen, "Hindered transport of large molecules in liquid-filled pores," *AIChE J.*, vol. 33, no. 9, pp. 1409–1425, 1987, doi: 10.1002/aic.690330902.

[44] F. G. Donnan, “Theory of membrane equilibria and membrane potentials in the presence of non-dialysing electrolytes. A contribution to physical-chemical physiology,” *J. Memb. Sci.*, vol. 100, no. 1, pp. 45–55, 1995, doi: https://doi.org/10.1016/0376-7388(94)00297-C.

[45] R. Kuhn, C. Vornholt, V. Preuß, I. M. Bryant, and M. Martienssen, “Aminophosphonates in nanofiltration and reverse osmosis permeates,” *Membranes (Basel).*, vol. 11, no. 6, pp. 1–16, 2021, doi: 10.3390/membranes11060446.

[46] J. Schaep and C. Vandecasteele, “Evaluating the charge of nanofiltration membranes,” *J. Memb. Sci.*, vol. 188, no. 1, pp. 129–136, 2001, doi: https://doi.org/10.1016/S0376-7388(01)00368-4.

[47] H. Zhang *et al.*, “Mineralization-inspired preparation of composite membranes with polyethyleneimine–nanoparticle hybrid active layer for solvent resistant nanofiltration,” *J. Memb. Sci.*, vol. 470, pp. 70–79, 2014, doi: https://doi.org/10.1016/j.memsci.2014.07.019.

[48] P. Daraei *et al.*, “Novel polyethersulfone nanocomposite membrane prepared by PANI/Fe 3O 4 nanoparticles with enhanced performance for Cu(II) removal from water,” *J. Memb. Sci.*, vol. 415–416, pp. 250–259, 2012, doi: 10.1016/j.memsci.2012.05.007.

[49] V. Vatanpour, M. Esmaeili, and M. H. D. A. Farahani, “Fouling reduction and retention increment of polyethersulfone nanofiltration membranes embedded by amine-functionalized multi-walled carbon nanotubes,” *J. Memb. Sci.*, vol. 466, pp. 70–81, 2014, doi: https://doi.org/10.1016/j.memsci.2014.04.031.

[50] D. K. F. Meijer and H. J. H. Geesink, “Favourable and Unfavourable EMF Frequency Patterns in Cancer: Perspectives for Improved Therapy and Prevention,” *J. Cancer Ther.*, vol. 09, no. 03, pp. 188–230, 2018, doi: 10.4236/jct.2018.93019.

[51] Y. Motarjemi, *Encyclopedia of Food Safety, 4v*. Burlington: Burlington Academic Press, 2014.

[52] M. Qtaishat, T. Matsuura, B. Kruczek, and M. Khayet, “Heat and mass transfer analysis in direct contact membrane distillation,” *Desalination*, vol. 219, no. 1–3, pp. 272–292, 2008, doi: 10.1016/j.desal.2007.05.019.

[53] S. Al-Asheh, F. Banat, M. Qtaishat, and M. Y. El-Khateeb, “Concentration of sucrose solutions via vacuum membrane distillation,” *Desalination*, vol. 195, no. 1–3, pp. 60–68, 2006, doi: 10.1016/j.desal.2005.10.036.

[54] K. Smolders and A. C. M. Franken, “Terminology for Membrane Distillation,” *Desalination*, vol. 72, no. 3, pp. 249–262, 1989, doi: https://doi.org/10.1016/0011-9164(89)80010-4.

[55] L. Martínez-Díez and M. I. Vázquez-González, “A method to evaluate coefficients affecting flux in membrane distillation,” *J. Memb. Sci.*, vol. 173, no. 2, pp. 225–234, 2000, doi: https://doi.org/10.1016/S0376-7388(00)00362-8.

[56] V. Holman, “Introduction,” *Vis. Resour.*, vol. 15, no. 3, pp. ix–x, 1999, doi: 10.1080/01973762.1999.9658510.

[57] Y. A. and ÇENGEL, *THERMODYNAMICS,AN ENGINEERING APPROACH*, vol. 1. 2019.

[58] M. Khayet, T. Matsuura, and J. I. Mengual, “Porous hydrophobic/hydrophilic composite membranes: Estimation of the hydrophobic-layer thickness,” *J. Memb. Sci.*, vol. 266, no. 1, pp. 68–79, 2005, doi: https://doi.org/10.1016/j.memsci.2005.05.012.

[59] K. W. Lawson and D. R. Lloyd, “Membrane distillation. II. Direct contact MD,” *J. Memb. Sci.*, vol. 120, no. 1, pp. 123–133, 1996, doi: https://doi.org/10.1016/0376-7388(96)00141-X.

[60] K. W. Lawson and D. R. Lloyd, “Membrane distillation,” *J. Memb. Sci.*, vol. 124, no. 1, pp. 1–25, 1997, doi: https://doi.org/10.1016/S0376-7388(96)00236-0.

[61] M. Klinko, K., Wilf, “Mark Wilf Ph. D. and Kenneth Klinko OPTIMIZATION OF SEAWATER RO SYSTEMS DESIGN.”

[62] L. I. M. Ayala *et al.*, “Water Defluoridation: Nanofiltration vs Membrane Distillation,” *Ind. Eng. Chem. Res.*, vol. 57, no. 43, pp. 14740–14748, 2018, doi: 10.1021/acs.iecr.8b03620.

[63] A. P. Padilla and H. Saitua, “Performance of simultaneous arsenic, fluoride and alkalinity (bicarbonate) rejection by pilot-scale nanofiltration,” *Desalination*, vol. 257, no. 1, pp. 16–21, 2010, doi: https://doi.org/10.1016/j.desal.2010.03.022.

[64] C. K. Diawara, “Nanofiltration process efficiency in water desalination,” *Sep. Purif. Rev.*, vol. 37, no. 3, pp. 302–324, 2008, doi: 10.1080/15422110802228770.

[65] L. F. Greenlee, D. F. Lawler, B. D. Freeman, B. Marrot, and P. Moulin, “Reverse osmosis desalination: Water sources, technology, and today’s challenges,” *Water Res.*, vol. 43, no. 9, pp. 2317–2348, 2009, doi: 10.1016/j.watres.2009.03.010.

[66] A. Shrivastava and D. Stevens, *Energy Efficiency of Reverse Osmosis*. Elsevier Inc., 2018.

[67] S. Chu and A. Majumdar, “Opportunities and challenges for a sustainable energy future,” *Nature*, vol. 488, no. 7411, pp. 294–303, 2012, doi: 10.1038/nature11475.

[68] P. O. lavagne; Taylor, “Energy Efficiency Indicators for Public Electricity Production from Fossil Fuels,” no. July, 2008.

[69] P. Ganesan, M. Thirugnanasambandam, S. Rajakarunakaran, and D. Devaraj, “Specific Energy Consumption and Co2 Emission Reduction Analysis in a Textile Industry,” *Int. J. Green Energy*, vol. 12, no. 7, pp. 685–693, Jul. 2015, doi: 10.1080/15435075.2013.829479.

[70] A. S. Stillwell and M. E. Webber, “Predicting the specific energy consumption of reverse osmosis desalination,” *Water (Switzerland)*, vol. 8, no. 12, pp. 1–18, 2016, doi: 10.3390/w8120601.

Appendix

Appendix 1:

```
clc
clear all
close all
%% reading excel data from the provided data
(Aalborg Universirty, Denmark)
doc_40 = xlsread('MD_water');
doc_50 = xlsread('MD_water','2'); % for 50 degree
values
doc_60 = xlsread('MD_water','3');% for 60 degree
values
%% we do the calculations for 60 degrees first
tbf_in = doc_60(2:13,3);% bulk feed in temp
tbf_out = doc_60(2:13,4); % bulf feed out temp
tbf = (tbf_in + tbf_out)*0.5; %  avg bulk feed
temp
tbp_in = doc_60(2:13,5); % bulk permeate in temp
tbp_out = doc_60(2:13,6);% bulk feed
tbp = (tbp_in + tbp_out)*0.5;
J = doc_60(2:13,9);% refes to flux in LMH
J = J/3600; % conversion from Kg/m2hr to Kg/m2s
flow = doc_60(2:13,8); % flow from the membrane
toward the other side in (ml/min)
flow = flow*0.000017; % unit conversion to kg/s
mf_in = (5.32*10^-3)*ones(12,1); % feed in mass
flow rate that is 19L/h
A = 0.1; %m2  membrane filtration area
rho = [989.547;988.8975;995.218;994.92];% rho =
[bf1;bf2;pf1;pf2]density
mf_out = vpa(mf_in - (J*A)); %vpa for increased
precision
%% reading enthalpy values for temperatures
h_in =
[233.6072;237.7912;238.2096;237.3728;238.2096;238.
2096;238.706;239.122;238.706;239.122;237.0064;237.
495];%for feed flow
h_in = h_in*1000; % Kg/Kj to j/kg
```

```
h_out =
[161.263;164.6054;167.53;170.8756;170.4574;175.057
6;176.3122;175.0576;177.985;181.3306;181.3306;180.
9124];%for feed flow
h_out = h_out*1000; % Kg/Kj to j/kg
% hin= [209.34;230.36;251.18];
% tin = [50;55;60];
% x(1) = (hin(1)*tbf_in(1)+tin(1)*hin(2)-
tbf_in(1)*hin(2)-hin(1)*tin(2))/(tin(1)-tin(2));
% for i=2:12
%     hin(i) = (hin(i-1)*tbf_in(i)+tin(i-
1)*hin(i+1)-tbf_in(i)*hin(i+1)-hin(i-
1)*tin(i+1))/(tin(i-1)-tin(i+1));
%     %if
% end
tbf_h_in = [];
tbf_h_in =
cat(1,tbf_h_in,[tbf_in(1:end),h_in(1:end)]);
tbf_h_out = [];
tbf_h_out =
cat(1,tbf_h_out,[tbf_out(1:end),h_out(1:end)]);
Hv =
[2388.84;2386.68;2385.72;2385;2384.44;2383.56;2383
.08;2383.32;2382.72;2381.512;2382.12;2381.512]; %
latent heat of vaporization
Hv = Hv*1000; % KJ/kg to J/kg
%% inputting known variables
kpa =
[0.162;0.163;0.1635;0.1639;0.164;0.1647;0.165;0.16
48;0.1652;0.1659;0.1655;0.1659]; % W/mk thermal
conductivity of membrane sheet for tbf (assumed
after consultation from literature)
kg =
[0.027;0.027;0.027;0.027;0.027;0.028;0.0283;0.0281
;0.0287;0.029;0.0289;0.029]; %W/mk thermal
conductivity of air trapped in membrane sheet
(assumed after consultation from literature)
e = 0.51 ; % porosity of membrane (assumed after
consultation from literature)
sigma_m = 450*10^-6; % thickness of membrane
(assumed after consultation from literature)
```

```
km = (e*kpa)+((1-e)*kg); %Wm/k combined thermal
conductivity of the membrane
hm = km/sigma_m; %W/m2K heat transfer coefficent
%% calculating heat transfer
Q_dot = (mf_in.*h_in) -(mf_out.*h_out); % heat
transfer inside the membrane
Q = Q_dot/A; % total heat that is transferred over
the unit area
%% calculation of evaporation efficicency
EE = (J.*Hv)./Q; % measure of efficiency of the
system
%% calculation of the unknowns from the fsolve
method for first 2 temperature values for tbf and
tbp
cp  = [4.1809;4.1811296;4.18002;4.179]; % cp =
[bf1;bf2;pf1;pf2]specific heat
cp  = cp*1000; %from KJ/Kg to J/kg
mew = [0.576767;0.567209;0.77408;0.763965]; % mew
=  [bf1;bf2;pf1;pf2] dynamic viscosity
mew = mew/1000 ; % from mPa.s to Pa.s
K = [637.1686;638.2522;616.7496;617.7338]; % K =
[bf1;bf2;pf1;pf2] thermal conductivity
K = K/1000; % from mW/mK to W/mk
C1 =
(K(2)/K(1))*(((rho(2)*mew(1))/(rho(1)*mew(2)))^0.6
4)*(((cp(2)*mew(2)*K(1))/(cp(1)*mew(1)*K(2)))^(1/3
));%*((mew(2)/mew(1))^0.14);
C2
=(K(4)/K(3))*(((rho(4)*mew(3))/(rho(3)*mew(4)))^0.
64)*(((cp(4)*mew(4)*K(3))/(cp(3)*mew(3)*K(4)))^(1/
3));%*((mew(3)/mew(3))^0.14);
%options =
optimoptions('fsolve','FinDiffType','central');
F = @MD;
XO =
[2.4*10^4;45;32.5;1.725*10^4;2.5*10^4;46;34;1.74*1
0^4];%initial guess
%Xt = zeroes(8,1);
X = fsolve(F,XO);
hf1 = X(1);
tmf1 = X(2);
```

```
tmp1 = X(3);
hp1 = X(4);
hf2 = X(5);
tmf2 = X(6);
tmp2 = X(7);
hp2 = X(8);
tb_avg = zeros(12,1);

%% Plotting of EE with average bulk and permeate
flow temperatures
for i=1:12
    tb_avg(i) = (tbf(i)+tbp(i))/2;
end
figure();

plot((tbp+tbf)/2,EE);
%% Calculation for the temperature polarization
coefficient
TPC1 = (tmf1-tmp1)/(tbf(1)-tbp(1));
TPC2 = (tmf2-tmp2)/(tbf(2)-tbp(2));
```

Appendix 2:

```
function Fun = MD(X)

Fun(1) =  X(1)*(47.15-X(2))-
3946.444881150000987823922571351 4 ;
Fun(2) = (213*(X(2)-X(3)) + (5.941666666666662e-
04*2388840))-3946.444881150000987823922571351 4;
Fun(3) = (X(4)*(X(3) - 31.6))-
3946.444881150000987823922571351 4;
Fun(4) = (X(5)*(48.05-X(6)))-
3999.931580072000463654952453040 9;
Fun(5) = (2.141333333333334e+02*(X(6)-X(7)) +
(0.000634000000000000*2386680))-
3999.931580072000463654952453040 9;
Fun(6) = X(8)*(X(7) - 32.35)-
3999.931580072000463654952453040 9;
Fun(7) = ((1.0059)- (X(5)/X(1)));%*((exp(-
6.4313+(1882/X(2)))/(exp(-
6.4313+(1882/X(6)))))^0.14));
Fun(8)= ((1.0048)-(X(8)/X(4)));%*((exp(-
6.4313+(1882/X(3)))/(exp(-
6.4313+(1882/X(7)))))^0.14));
end
```

Appendix 3:

```
%% THE nano-filtration
% the membrane used is NF 90
% Experimental Data

%w_i = 2; %water_input = 2L irrelevant
delta_p =linspace(0.01,1);% transmembrane pressure
=  bar
delta_p = (delta_p*100000)';
prompt = 'input starting value for feed flow rate
in m^3/s ';
a = input(prompt);
prompt2 = 'input ending value for feed flow rate
in m^3/s ';
b = input(prompt2);
Qf = linspace(a,b);
prompt3 = 'input the value for permeate flow rate
in m3/s';
Qp = input(prompt3);
%Qp = (1.9347*10^-3) * Qf; %70 percent of Qf is
the permeate flow rate.(supposed)
%% Safe/backup plan code
% Q_f = 3.83*10^-6; %m^3/s feed flow rate
4.91*10^-6
% Q_p = 7.41*10^-9; %m^3/s permeate flow rate
%% New SEC calculation

for i = 1:100
    for j =1:100
    x(i,j) = delta_p(i).*Qf(j); % with row the
pressure changes
      y(i,j) = x(i,j)/Qp;        % with column the
Q_f changes
    end
end
 SEC = (2.778*10^-7).*y;
%%
% SEC = (2.778*10^-7)*((delta_p*Q_f)/Q_p);
%specific energy consumption formula in KWH/m^3
 plot((delta_p/100000),SEC);
```

```
 title('Delta P vs SEC value');
 xlabel('Delta_P, (bar)');
 ax.XLim = [0 , 1];
 yticks(0:1:20);
 xticks(0:.1:1);
ylabel('SEC (KWH/m^3)');
%% SEC value should produce a lower cost as
compared to italian GOV cost.
cost_KWH = 0.15; %  price euro/KWH
specific_price = cost_KWH * SEC; %euro/m3
figure()
plot(SEC,specific_price);
ylabel('price (euro/m^3)');
xlabel('SEC (KWH/m^3)');
yticks(0:.25:2.5);
xticks(0:1:18);
```

Appendix 4:

Graphs for membrane distillation for flux and water recovery for Membrane Distillation.

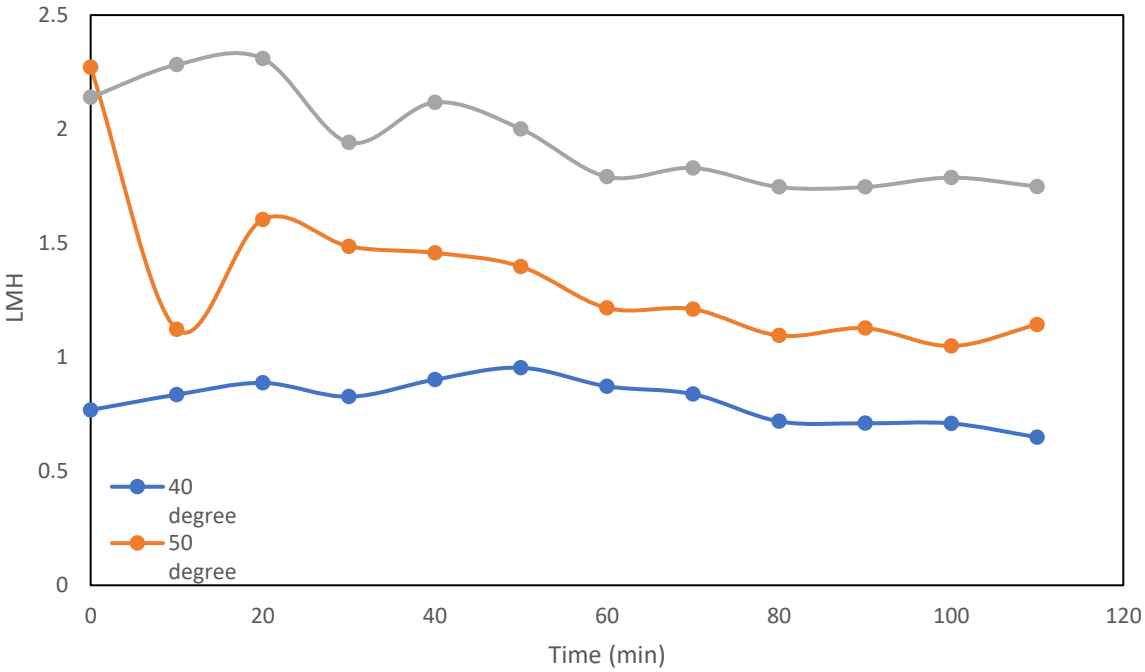

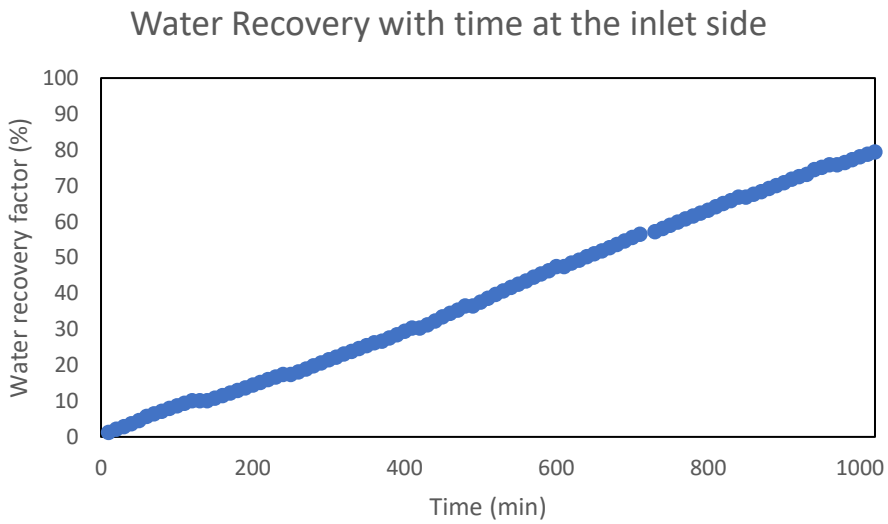

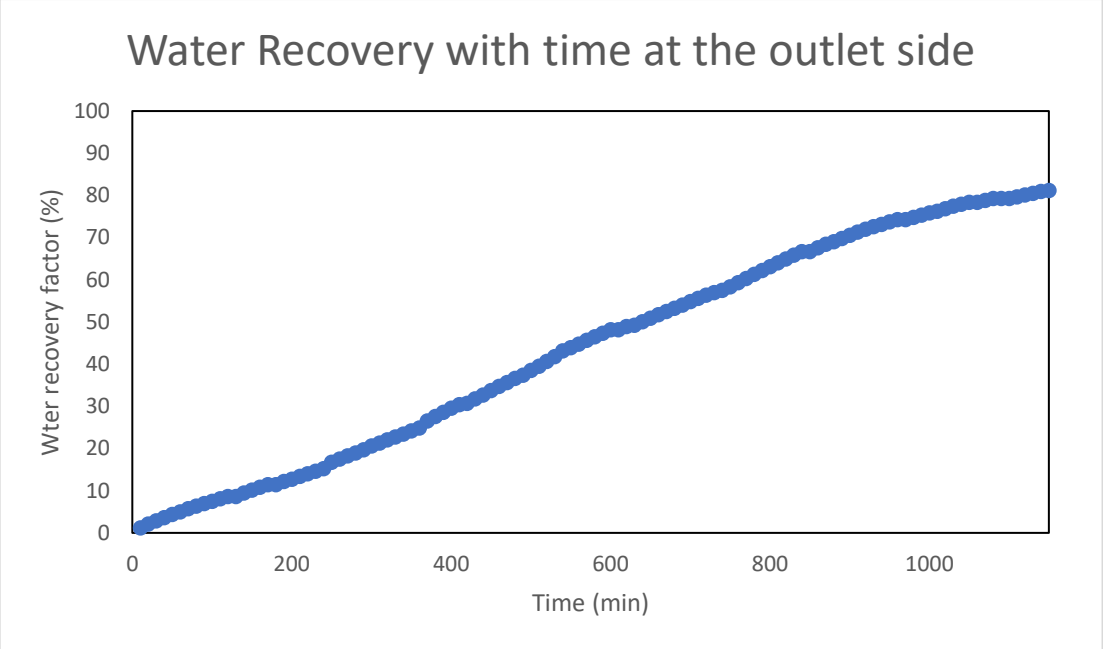
Water Recovery with time at the outlet side
Wter recovery factor (%)
100
90
80
70
60
50
40
30
20
10
0
0
200
400
600
800
1000
Time (min)